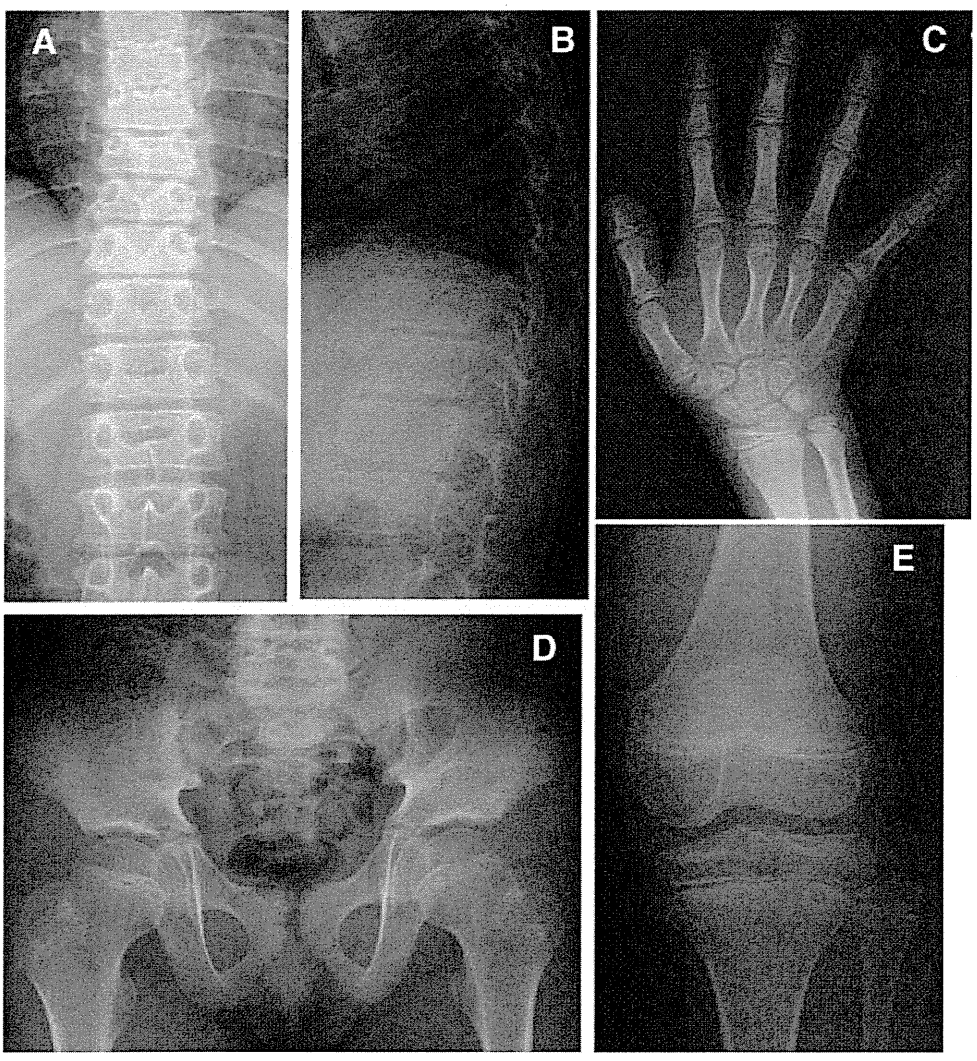

Figure 3 Radiographs of P5 at age 8 years 8 months. (A) Spine anteroposterior (AP). Platyspondyly. Over-faced pedicle is not so distinct. (B) Spine lateral. Flattened vertebral bodies and narrow disc spaces. (C) The right hand AP. Slightly short metacarpals. Phalanges are not so short. The bone age is advanced (12 years by the Greulich-Pyle method). (D) Pelvis AP. Short femoral neck and horizontal acetabulum. Proximal epiphyses are normal. (E) The right knee AP. Unremarkable changes. No fibula overgrowth.

predicted to create a premature stop codon (p.A113GfsX18), thereby most probably resulting in a null allele due to nonsense mutation mediated RNA decay (NMD).[11] The mutation was not found in the public mutation database and sequence variation database. Also, it was not found in 93 ethnically matched controls examined by Invader assay.[10]

Identification of *PAPSS2* mutations in sporadic cases

We screened for *PAPSS2* mutations in P4-6 by direct sequencing as previously described.[9] We found *PAPSS2* mutations in both chromosomes of all subjects (table 2). All mutations are predicted to create premature stop codons before the second last exon of the gene. Therefore, they are most likely to result in null alleles due to NMD. P5 was a homozygote, and P4 and P6 were heterozygotes for the mutations. Compound heterozygosity of the subjects was confirmed by sequencing of the parents' genomic DNA. All these mutations were not found in 93 ethnically matched controls examined by Invader assay[10] nor in public databases.

Phenotypes of the patients with *PAPSS2* mutations

Clinical features of our six patients were short-trunk short stature with short neck (table 1). The short stature was noticeable early in life, but not always at birth; it usually became definite after age 5–6 years. All patients had normal intelligence and facies. Corneal opacity was not found. Kyphosis and/or scoliosis were found in three subjects. Bone age was advanced in all (4/4) cases evaluated. No clinical sign of androgen excess was noted in all (6/6) patients and their family members. The main radiographic feature was pronounced flattening of spine (rectangular vertebral body), particularly in the thoracic spine, which accompanied irregular

Table 2 *PAPSS2* mutations in autosomal recessive brachyolmia

Family	Exon	Nucleotide change	Amino acid change
1	3	c.337_338insG (homozygous)	p.A113GfsX18
2	5	c.616-634del19	p.V206SfsX9
	11	c.1309-1310delAG	p.R437GfsX19
3	3	IVS3+2delT (homozygous)	p.L50SfsX2
4	4	c.480_481insCGTA	p.K161RfsX6
	6	c.661delA	p.I221SfsX40

The nucleotide changes are shown with respect to *PAPSS2* mRNA sequence (NM_001015880). The corresponding predicted amino acid changes are numbered from the initiating methionine residue. Exons are numbered sequentially 1–13.

endplates and narrow disc spaces. Mild shortening of the femoral neck and metacarpals were common features. The costal cartilages showed precocious calcification in the adult subjects (3/3). Epiphyseal and metaphyseal dysplasias were very mild, if present. From these features of spine predominant dysplasia, our patients can be diagnosed as having brachyolmia. Among known types of brachyolmias, characteristics of the Hobaek and Toledo types are mixed.[1 4]

DISCUSSION

PAPSS2 mutation has been reported to be responsible for two other overlapping, but distinct, phenotypes. The first is SEMD Pakistani type; Ahmad *et al*[12] described a large consanguineous Pakistani family with a distinct form of SEMD with autosomal inheritance. Its clinical features include short stature evident at birth, short and bowed lower limbs, mild brachydactyly, kyphoscoliosis, enlarged knee joints, and precocious osteoarthropathy. Radiographic features are platyspondyly with irregular endplates and narrowed joint spaces, delayed epiphyseal ossification at the hips and knees, diffuse early osteoarthritic changes primarily in the spine and hands, and mild brachydactyly. Metaphyseal abnormalities are seen predominantly in the hips and knees. This disease is differentiated from other forms of SEMD by its mild degree of metaphyseal involvement, type of brachydactyly, and the absence of loose joints or other clinical findings. A homozygous nonsense mutation of *PAPSS2* (S438X) is identified in all affected individuals in the family.[13] Many of the characteristics of SEMD Pakistani type, including enlarged joints with deformity, delayed epiphyseal ossification at the hips and knees, and precocious osteoarthritic changes of the large and small joints, are absent in our cases (table 1).

PAPSS2 mutations have also been found in a patient with a different phenotype, spondylodysplasia and premature pubarche.[9] A Turkish girl with premature pubarche, hyperandrogenic anovulation, short stature, and skeletal dysplasia showed a compound heterozygosity for a missense and a nonsense mutation in *PAPSS2*: the former was a 143C>G transversion resulting in a T48R substitution at a conserved residue in the adenosine 5-prime-phosphosulfate kinase domain, and the latter was a 985C>T transition resulting in R329X. Their functional assays revealed no detectable activity for R329X, and only minor residual activity for T48R (6% of the wild type activity). The mother who carried the R329X mutation had normal pubarche and menarche, but developed obesity, oligomenorrhoea, and hirsutism in her fourth decade, while the father who carried the T48R mutation showed normal growth and pubertal development. The skeletal changes in this patient are more similar to those of our cases than SEMD Pakistani type (table 1).

Among our patients, spinal changes were very similar, but epiphyseal and metaphyseal changes were considerably variable (table 1). P4 and P5, similar to the case reported by Noordam *et al*,[9] showed minimal epiphyseal and metaphyseal dysplasias. P6 had considerable epi-metaphyseal changes in the long bones of the lower extremities; they were more severe than those in family 1 (P1-3), but were far milder than those in SEMD Pakistani type. The differential diagnosis includes AR spondyloepiphyseal dysplasia tarda[14] because of late manifestation, AR inheritance, and relatively mild spondyloepiphyseal dysplasia with flat vertebral bodies with irregular endplates. In the disorder, overfaced vertebral bodies is absent and the capital femoral epiphyses are severely affected.[14]

In a form of autosomal dominant brachyolmia, heterozygous *TRPV4* mutation has been identified.[5 6] Notably, the *TRPV4* mutation presents a wide phenotypic gradation from brachyolmia at its most mild, through spondylometaphyseal dysplasia type Kozlowski, spondyloepiphyseal dysplasia type Maroteaux, and metatropic dysplasia, to parastremmatic dysplasia and fetal akinesia at its most severe.[5 15–17] *PAPSS2* mutations might also present a phenotype gradation from brachyolmia to spondylo-epiphyseal and spondylo-epimetaphyseal dysplasia like SEMD Pakistani type. Further investigation of *PAPSS2* mutations in brachyolmia and skeletal dysplasias with overlapping phenotypes to our cases as well as other cases with *PAPSS2* mutations[9 14] would provide further answers.

An additional supplementary table is published online only. To view this file please visit the journal online (http://jmg.bmj.com)

Acknowledgements We thank the patients and their family for their help to the study. We also thank the Japanese Skeletal Dysplasia Consortium.

Contributors NM performed the exome experiments, analysed the data, wrote the paper, and is guarantor. NE and PI collected family samples and evaluated their phenotypes. AI performed the sequence experiments, analysed the data, and wrote the paper. JD performed the experiments. NoM, KM, TC, OK, and TN collected samples and evaluated their clinical and radiographic phenotypes. TH and GN analysed the clinical data. HO collected and controlled the experimental samples. NaM performed the experiments and analysed the data. SI analysed the data, wrote the paper, and is also guarantor. All authors have critically revised the paper.

Funding This study is supported by research grants from the Ministry of Health, Labour and Welfare (23300101: S Ikegawa and N Matsumoto; 23300102: T Hasegawa; 23300201: S Ikegawa), by a Grant-in-Aid for Young Scientists from the Japan Society for the Promotion of Science (N Miyake), and by Research on intractable diseases, Health and Labour Sciences Research Grants, H23-Nanchi-Ippan-123 (S Ikegawa).

Patient consent Obtained.

Ethics approval This study was performed under the approval of the ethical committee of RIKEN, Yokohama City University, and participating institutions.

Provenance and peer review Not commissioned; externally peer reviewed.

Data sharing statement Additional unpublished data on mutation examination are available on request to researchers.

REFERENCES

1. **Shohat M,** Lachman R, Gruber HE, Rimoi DL. Brachyolmia: radiographic and genetic evidence of heterogeneity. *Am J Med Genet* 1989;**33**:209–19.
2. **Kozlowski K,** Beemer FA, Bens G, Dijkstra PF, Iannaccone G, Emons D, Lopez-Ruiz P, Masel J, van Nieuwenhuizen O, Rodriguez-Barrionuevo C. Spondylo-Metaphyseal Dysplasia (Report of 7 cases and essay of classification). *Prog Clin Biol Res* 1982;**104**:89–101.
3. **McKusick VA.** Medical genetics. A 40-year perspective on the evolution of a medical specialty from a basic science. *JAMA* 1993;**270**:2351–6.
4. **Hoo JJ,** Oliphant M. Two sibs with brachyolmia type Hobaek: five year follow-up through puberty. *Am J Med Genet A* 2003;**116A**:80–4.
5. **Rock MJ,** Prenen J, Funari VA, Funari TL, Merriman B, Nelson SF, Lachman RS, Wilcox WR, Reyno S, Quadrelli R, Vaglio A, Owsianik G, Janssens A, Voets T, Ikegawa S, Nagai T, Rimoin DL, Nilius B, Cohn DH. Gain-of-function mutations in TRPV4 cause autosomal dominant brachyolmia. *Nat Genet* 2008;**40**:999–1003.
6. **Dai J,** Cho TJ, Unger S, Lausch E, Nishimura G, Kim OH, Superti-Furga A, Ikegawa S. TRPV4-pathy, a novel channelopathy affecting diverse systems. *J Hum Genet* 2010;**55**:400–2.
7. **Doi H,** Yoshida K, Yasuda T, Fukuda M, Fukuda Y, Morita H, Ikeda S, Kato R, Tsurusaki Y, Miyake N, Saitsu H, Sakai H, Miyatake S, Shiina M, Nukina N, Koyano S, Tsuji S, Kuroiwa Y, Matsumoto N. Exome sequencing reveals a homozygous SYT14 mutation in adult-onset, autosomal-recessive spinocerebellar ataxia with psychomotor retardation. *Am J Hum Genet* 2011;**89**:320–7.
8. **Tsurusaki Y,** Okamoto N, Ohashi H, Kosho T, Imai Y, Hibi-Ko Y, Kaname T, Naritomi K, Kawame H, Wakui K, Fukushima Y, Homma T, Kato M, Hiraki Y, Yamagata T, Yano S, Mizuno S, Sakazume S, Ishii T, Nagai T, Shiina M, Ogata K, Ohta T, Niikawa N, Miyatake S, Okada I, Mizuguchi T, Doi H, Saitsu H, Miyake N, Matsumoto N. Mutations affecting components of the SWI/SNF complex cause Coffin-Siris syndrome. *Nat Genet* 2012;**44**:376–8.
9. **Noordam C,** Dhir V, McNelis JC, Schlereth F, Hanley NA, Krone N, Smeitink JA, Smeets R, Sweep FC, Claahsen-van der Grinten HL, Arlt W. Inactivating PAPSS2 mutations in a patient with premature pubarche. *N Engl J Med* 2009;**360**:2310–18.

10. **Ohnishi Y,** Tanaka T, Ozaki K, Yamada R, Suzuki H, Nakamura Y. A high-throughput SNP typing system for genome-wide association studies. *J Hum Genet* 2001;**46**:471–7.
11. **Holbrook JA,** Neu-Yilik G, Hentze MW, Kulozik AE. Nonsense-mediated decay approaches the clinic. *Nat. Genet* 2004;**36**:801–8.
12. **Ahmad M,** Haque MF, Ahmad W, Abbas H, Haque S, Krakow D, Rimoin DL, Lachman RS, Cohn DH. Distinct, autosomal recessive form of spondyloepimetaphyseal dysplasia segregating in an inbred Pakistani kindred. *Am J Med Genet* 1998;**78**:468–73.
13. **Faiyaz ul Haque M,** King LM, Krakow D, Cantor RM, Rusiniak ME, Swank RT, Superti-Furga A, Haque S, Abbas H, Ahmad W, Ahmad M, Cohn DH. Mutations in orthologous genes in human spondyloepimetaphyseal dysplasia and the brachymorphic mouse. *Nat Genet* 1998;**20**:157–62.
14. **Leroy JG,** Leroy BP, Emmery LV, Messiaen L, Spranger JW. A new type of autosomal recessive spondyloepiphyseal dysplasia tarda. *Am J Med Genet A* 2004;**125A**:49–56.
15. **Krakow D,** Vriens J, Camacho N, Luong P, Deixler H, Funari TL, Bacino CA, Irons MB, Holm IA, Sadler L, Okenfuss EB, Janssens A, Voets T, Rimoin DL, Lachman RS, Nilius B, Cohn DH. Mutations in the gene encoding the calcium-permeable ion channel TRPV4 produce spondylometaphyseal dysplasia, Kozlowski type and metatropic dysplasia. *Am J Hum Genet* 2009;**84**:307–15.
16. **Nishimura G,** Dai J, Lausch E, Unger S, Megarbané A, Kitoh H, Kim OH, Cho TJ, Bedeschi F, Benedicenti F, Mendoza-Londono R, Silengo M, Schmidt-Rimpler M, Spranger J, Zabel B, Ikegawa S, Superti-Furga A. Spondylo-epiphyseal dysplasia, Maroteaux type (pseudo-Morquio syndrome type 2), and parastremmatic dysplasia are caused by TRPV4 mutations. *Am J Med Genet A* 2010;**152A**:1443–9.
17. **Unger S,** Lausch E, Stanzial F, Gillessen-Kaesbach G, Stefanova I, Di Stefano CM, Bertini E, Dionisi-Vici C, Nilius B, Zabel B, Superti-Furga A. Fetal akinesia in metatropic dysplasia: The combined phenotype of chondrodysplasia and neuropathy? *Am J Med Genet A* 2011;**155A**:2860–4.

PLOS ONE

Molecular and Clinical Studies in 138 Japanese Patients with Silver-Russell Syndrome

Tomoko Fuke[1,2], Seiji Mizuno[3], Toshiro Nagai[4], Tomonobu Hasegawa[2], Reiko Horikawa[5], Yoko Miyoshi[6], Koji Muroya[7], Tatsuro Kondoh[8], Chikahiko Numakura[9], Seiji Sato[10], Kazuhiko Nakabayashi[11], Chiharu Tayama[11], Kenichiro Hata[11], Shinichiro Sano[1,12], Keiko Matsubara[1], Masayo Kagami[1], Kazuki Yamazawa[1], Tsutomu Ogata[1,12]*

1 Department of Molecular Endocrinology, National Research Institute for Child Health and Development, Tokyo, Japan, **2** Department of Pediatrics, Keio University School of Medicine, Tokyo, Japan, **3** Department of Pediatrics, Central Hospital, Aichi Human Service Center, Aichi, Japan, **4** Department of Pediatrics, Dokkyo Medical University Koshigaya Hospital, Saitama, Japan, **5** Division of Endocrinology and Metabolism, National Center for Child Health and Development, Tokyo, Japan, **6** Department of Pediatrics, Osaka University Graduate School of Medicine, Suita, Japan, **7** Department of Endocrinology and Metabolism, Kanagawa Children's Medical Center, Kanagawa, Japan, **8** Division of Developmental Disability, Misakaenosono Mutsumi Developmental, Medical, and Welfare Center, Isahaya, Japan, **9** Department of Pediatrics, Yamagata University School of Medicine, Yamagata, Japan, **10** Department of Pediatrics, Saitama Municipal Hospital, Saitama, Japan, **11** Department of Maternal-Fetal Biology, National Research Institute for Child Health and Development, Tokyo, Japan, **12** Department of Pediatrics, Hamamatsu University School of Medicine, Hamamatsu, Japan

Abstract

Background: Recent studies have revealed relative frequency and characteristic phenotype of two major causative factors for Silver-Russell syndrome (SRS), i.e. epimutation of the *H19*-differentially methylated region (DMR) and uniparental maternal disomy 7 (upd(7)mat), as well as multilocus methylation abnormalities and positive correlation between methylation index and body and placental sizes in *H19*-DMR epimutation. Furthermore, rare genomic alterations have been found in a few of patients with idiopathic SRS. Here, we performed molecular and clinical findings in 138 Japanese SRS patients, and examined these matters.

Methodology/Principal Findings: We identified *H19*-DMR epimutation in cases 1–43 (group 1), upd(7)mat in cases 44–52 (group 2), and neither *H19*-DMR epimutation nor upd(7)mat in cases 53–138 (group 3). Multilocus analysis revealed hyper- or hypomethylated DMRs in 2.4% of examined DMRs in group 1; in particular, an extremely hypomethylated *ARHI*-DMR was identified in case 13. Oligonucleotide array comparative genomic hybridization identified a ~3.86 Mb deletion at chromosome 17q24 in case 73. Epigenotype-phenotype analysis revealed that group 1 had more reduced birth length and weight, more preserved birth occipitofrontal circumference (OFC), more frequent body asymmetry and brachydactyly, and less frequent speech delay than group 2. The degree of placental hypoplasia was similar between the two groups. In group 1, the methylation index for the *H19*-DMR was positively correlated with birth length and weight, present height and weight, and placental weight, but with neither birth nor present OFC.

Conclusions/Significance: The results are grossly consistent with the previously reported data, although the frequency of epimutations is lower in the Japanese SRS patients than in the Western European SRS patients. Furthermore, the results provide useful information regarding placental hypoplasia in SRS, clinical phenotypes of the hypomethylated *ARHI*-DMR, and underlying causative factors for idiopathic SRS.

Citation: Fuke T, Mizuno S, Nagai T, Hasegawa T, Horikawa R, et al. (2013) Molecular and Clinical Studies in 138 Japanese Patients with Silver-Russell Syndrome. PLoS ONE 8(3): e60105. doi:10.1371/journal.pone.0060105

Editor: Monica Miozzo, Università degli Studi di Milano, Italy

Received September 7, 2012; **Accepted** February 21, 2013; **Published** March 22, 2013

Funding: This work was funded by Grants-in-Aid for Scientific Research (A) (22249010) and Research (B) (21028026) from the Japan Society for the Promotion of Science (http://www.jsps.go.jp/english/index.html), by Grant for Research on Rare and Intractable Diseases (H24-042) from the Ministry of Health, Labor and Welfare (http://www.mhlw.go.jp/english/), and by Grant for National Center for Child Health and Development (23A-1) (http://www.ncchd.go.jp/English/Englishtop.htm). The funders had no role in study design, data collection and analysis, decision to publish, or preparation of the manuscript.

Competing Interests: The authors have declared that no competing interests exist.

* E-mail: tomogata@hama-med.ac.jp

Introduction

Silver-Russell syndrome (SRS) is a rare congenital developmental disorder characterized by pre- and postnatal growth failure, relative macrocephaly, triangular face, hemihypotrophy, and fifth-finger clinodactyly [1]. Recent studies have shown that epimutation (hypomethylation) of the paternally derived differentially methylated region (DMR) in the upstream of *H19* (*H19*-DMR) on chromosome 11p15.5 and maternal uniparental disomy for chromosome 7 (upd(7)mat) account for ~45% and 5–10% of SRS patients, respectively [1,2]. In this regard, phenotypic assessment has suggested that birth length and weight are more reduced and characteristic body features are more frequent in patients with *H19*-DMR epimutation than in those with upd(7)mat, whereas developmental delay tends to be more

frequent in patients with upd(7)mat than in those with *H19*-DMR epimutation [3,4]. Furthermore, consistent with the notion that imprinted genes play an essential role in placental growth and development [5], placental hypoplasia has been found in both *H19*-DMR epimutation and upd(7)mat [4,6], although comparison of placental weight has not been performed between *H19*-DMR hypomethylation and upd(7)mat. In addition, multilocus hypo- or hypermethylation and positive correlation between methylation index (MI, the ratio of methylated clones) and body and placental sizes have been reported in patients with *H19*-DMR epimutation [4,7–9], and several types of rare genomic alterations have been identified in a few of SRS patients [1,10–12].

Here, we report on molecular and clinical findings in 138 Japanese SRS patients, and discuss on the results obtained in this study.

Patients and Methods

Ethics statement

This study was approved by the Institutional Review Board Committee at the National Center for Child Health and Development. The parents of the affected children and the adult patients who can express an intention by themselves have given written informed consent to participate in this study and to publish their molecular and clinical data.

Patients

This study consisted of 138 Japanese patients (66 males and 72 females) with SRS phenotype aged 0–30 years (median 4.1 years), including 64 previously reported patients (20 patients with variable degrees of *H19*-DMR epimutation, three patients with upd(7)mat, one patient with 46,XY/46,XY,upd(7)mat mosaicism in whom upd(7)mat cells accounted for 91–92% of leukocytes and salivary cells and for 11% of placental tissue, and 40 patients of unknown cause) [4,6,13]. The 138 patients had a normal karyotype in all the ≥50 lymphocytes examined, and satisfied the selection criteria proposed by Netchine et al. [14], i.e., birth length and/or birth weight ≤ −2 standard deviation score (SDS) for gestational age as a mandatory criteria plus at least three of the following five features: (i) postnatal short stature (≤ −2 SDS) at 2 year of age or at the nearest measure available, (ii) relative macrocephaly at birth, i.e., SDS for birth length or birth weight minus SDS for birth occipitofrontal circumference (OFC) ≤ −1.5, (iii) prominent forehead during early childhood, (iv) body asymmetry, and (v) feeding difficulties during early childhood. Birth and present length/height, weight, and OFC were assessed by the gestational/postnatal age- and sex-matched Japanese reference data from the Ministry of Health, Labor, and Welfare and the Ministry of Education, Science, Sports and Culture. Placental weight was assessed by the gestational age-matched Japanese reference data [15]. Clinical features were evaluated by clinicians at different hospitals who participated in this study, using the same clinical datasheet. The SRS patients were classified into three groups by the molecular studies, i.e., those with *H19*-DMR hypomethylation (epimutation) (group 1), those with upd(7)mat (group 2), and the remaining patients (group 3).

Primers and samples

Primers utilized in this study are shown in Table S1. Leukocyte genomic DNA samples were examined in this study.

Methylation analysis

We performed pyrosequencing analysis for the *H19*-DMR encompassing the 6th CTCF (CCCTC-binding factor) binding site that functions as the primary regulator for the monoallelic *IGF2* and *H19* expressions [16–18], using bisulfite treated leukocyte genomic DNA samples of all the 138 patients. The procedure was as described in the manufacturer's instructions (Qiagen, Valencia, CA, USA). In brief, a 279 bp region was PCR-amplified with a primer set (PyF and PyR) for both methylated and unmethylated clones, and a sequence primer (SP) was hybridized to a single-stranded PCR products. Subsequently, the MIs were obtained for four CpG dinucleotides (CG5–CG7 and CG9), using PyroMark Q24 (Qiagen) (the MI for CG8 was not obtained, because the "C" residue of CG8 constitutes a C/T SNP) (Figure 1A). The PyF/PyR and SP were designed by PyroMark Assay Design Software Ver2.0. While the PyF sequence contains a SNP (*rs11564736*) with a mean minor allele frequency of 5% in multiple populations, the minor allele frequency is 0% in the Japanese as well as in the Asian populations (http://browser.1000genomes.org/Homo_sapiens/Variation/Population?db=core;r=11:2020801–2021801;v=rs11564736;vdb=variation;vf=7864021). Thus, we utilized this PyF.

We also carried out combined bisulfite restriction analysis (COBRA) for the *H19*-DMR. The methods were as described previously [4]. In short, a 435 bp region was PCR-amplified with a primer set (CoF and CoR) that hybridize to both methylated and unmethylated clones, and MIs were obtained for two CpG dinucleotides (CG5 and CG16) after digestion of the PCR products with methylated allele-specific restriction enzymes (*Hpy*188I and *Afl*III) (Figure 1A).

Thus, we could examine CG5 by both pyrosequencing and COBRA. While we also attempted to analyze CG16 by both methods, it was impossible to design an SP for the analysis of CG16 (although we could design an SP between CG11 and CG12, clear methylation data were not obtained for CG16, probably because of the distance between the SP and CG16).

In addition, we performed COBRA for the KvDMR1 in all the 138 patients (Figure S1A) because of the possibility that epimutation of the KvDMR1 could lead to SRS phenotype via some mechanism(s) such as overexpression of a negative growth regulator *CDKN1C* [19], and for multiple DMRs on various chromosomes in patients in whom relatively large amount of DNA samples were available, as reported previously [4,20,21]. To define the reference ranges of MIs (minimum ~ maximum), 50 control subjects were similarly studied with permission.

To screen upd(7)mat, PCR amplification was performed for the *MEST*-DMR on chromosome 7q32.2 in all the 138 patients, using methylated and unmethylated allele-specific PCR primer sets, as reported previously [6] (Figure 2A). In addition, bisulfite sequencing and direct sequencing for the primer binding sites for the *ARHI*-DMR analysis were performed in a patient (case 13) with an extremely low MI for the *ARHI*-DMR.

Microsatellite analysis

Microsatellite analysis was performed for four loci within a ~4.5 Mb telomeric 11p region (*D11S2071*, *D11S922*, *D11S1318*, and *D11S988*) in patients with hypomethylated *H19*-DMR, to examine the possibility of upd(11p)mat involving the *H19*-DMR. Microsatellite analysis was also carried out for nine loci widely dispersed on chromosome 7 (Table S2) in patients with abnormal methylation patterns of the *MEST*-DMR, to examine the possibility of upd(7)mat and to infer the underlying causes for upd(7)mat, i.e., trisomy rescue, gamete complementation, monosomy rescue, and post-fertilization mitotic error [22]. The methods have been reported previously [4,6].

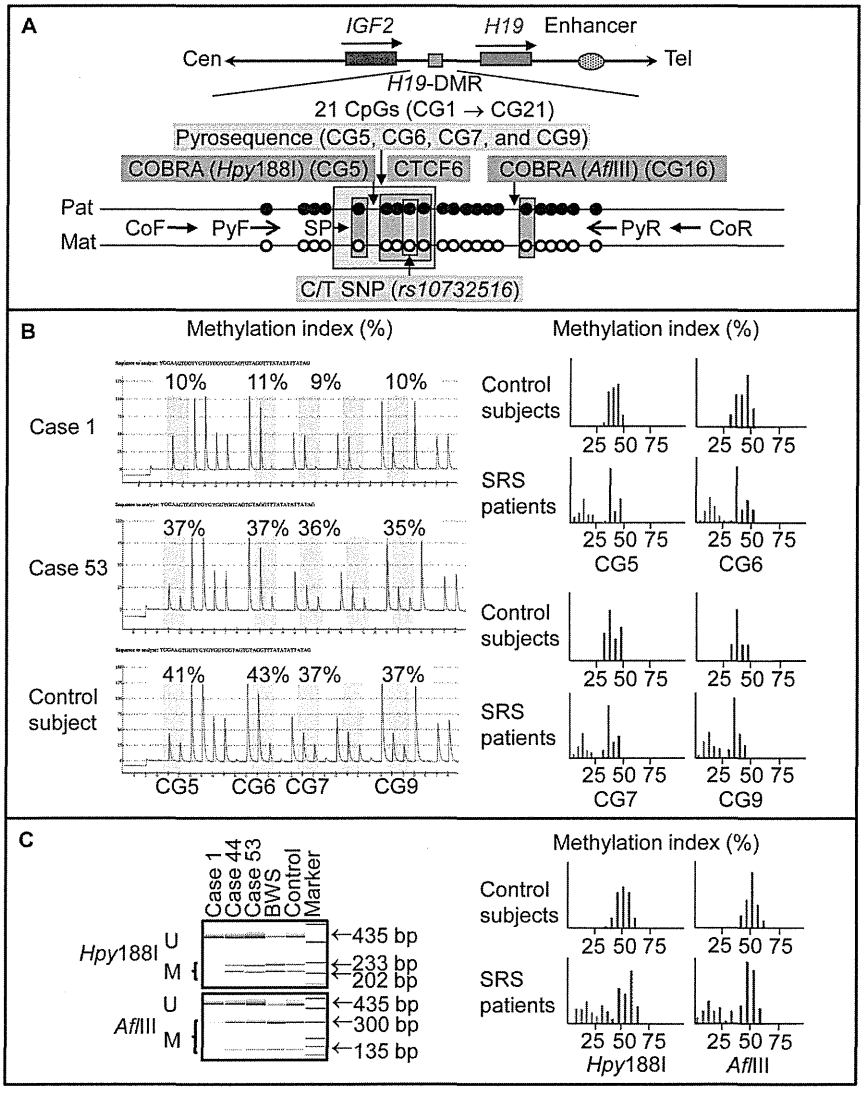

Figure 1. Methylation analysis of the *H19*-DMR, using bisulfite-treated genomic DNA. A. Schematic representation of a segment encompassing 21 CpG dinucleotides (CG1→CG21) within the *H19*-DMR. The cytosine residues at the CpG dinucleotides are usually methylated after paternal transmission (filled circles) and unmethylated after maternal transmission (open circles). The CTCF binding site 6 (CTCF6) is indicated with a blue rectangle; the cytosine residue at CG8 constitutes a C/T SNP (indicated with a gray rectangle). For pyrosequencing analysis, a 279 bp segment was PCR-amplified with PyF & PyR primers, and a sequence primer (SP) was hybridized to a single-stranded PCR products. Subsequently, the MIs were obtained for four CpG dinucleotides (CG5–CG7 and CG9) (indicated with a yellow rectangle). For COBRA, a 435 bp region was PCR-amplified with CoF & CoR primers, and the PCR product was digested with methylated allele-specific restriction enzymes to examine the methylation pattern of CG5 ands CG16 (the PCR products is digested with *Hpy*188I when the cytosine residue at CG5 is methylated and with *Afl*III when the cytosine residue at CG16 is methylated) (indicated with orange rectangles). *IGF2* is a paternally expressed gene, and *H19* is a maternally expressed gene. The stippled ellipse indicates the enhancer for *IGF2* and *H19*. B. Pyrosequencing data. Left part: Representative results indicating the MIs for CG5– CG7 and CG9. CG5– CG7 and CG9 are hypomethylated in case 1, and similarly methylated between case 53 and a control subject. Right part: Histograms showing the distribution of the MIs (the horizontal axis: the methylation index; and the vertical axis: the patient number). Forty-three SRS patients with low MIs are shown in red. C. COBRA data. Left part: Representative findings of PCR products loaded onto a DNA 1000 LabChip (Agilent, Santa Clara, CA, USA) after digestion with *Hpy*188I or *Afl*III. U: unmethylated clone specific bands; M: methylated clone specific bands; and BWS: Beckwith-Wiedemann syndrome patient with upd(11p15)pat. Right part: Histograms showing the distribution of the MIs.
doi:10.1371/journal.pone.0060105.g001

Oligoarray comparative genomic hybridization (CGH)

We performed oligoarray CGH in the 138 SRS patients, using a genomewide 4×180K Agilent platform catalog array and a custom-build high density oligoarray for the 11p15.5, 7p12.2, 12q14, and 17q24 regions where rare copy number variants have been identified in several SRS patients [1,10–12] as well as for the 7q32–qter region involved in the segmental upd(7)mat in four SRS patients [23–25]. The custom-build high density oligoarray contained 3,214 probes for 7p12.2, 434 probes for 7q32, 23,162 probes for 12q14, and 39,518 probes for 17q24, together with ~10,000 reference probes for other chromosomal region (Agilent Technologies, Palo Alto, CA, USA). The procedure was as described in the manufacturer's instructions.

Statistical analysis

After examining normality by χ^2 test, the variables following the normal distribution were expressed as the mean±SD, and those not following the normal distribution were expressed with the

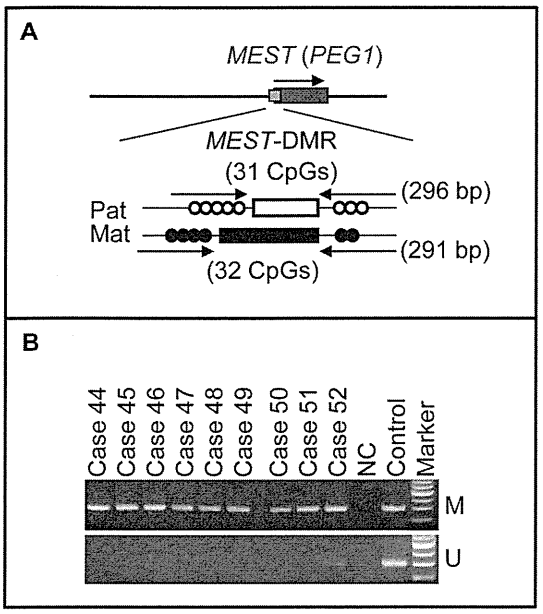

Figure 2. Methylated and unmethylated allele-specific PCR analysis for the *MEST*-DMR. A. Schematic representation of the *MEST*-DMR. The cytosine residues at the CpG dinucleotides are usually unmethylated after paternal transmission (open circles) and methylated after maternal transmission (filled circles). The PCR primers have been designed to hybridize either methylated or unmethylated clones. B. The results of methylation analysis with methylated and unmethylated allele-specific primers.
doi:10.1371/journal.pone.0060105.g002

median and range. Statistical significance of the mean was analyzed by Student's *t*-test or Welch's *t*-test after comparing the variances by *F* test, that of the median by Mann-Whitney's *U*-test, that of the frequency by Fisher's exact probability test, and that of the correlation by Pearson's correlation coefficient after confirming the normality of the variables. $P<0.05$ was considered significant.

Results

Identification of *H19*-DMR hypomethylation

Representative findings are shown in Figure 1B and 1C, and the MIs are summarized in Table 1. Overall, the MIs obtained by the pyrosequencing analysis tended to be lower and distributed more narrowly than those obtained by the COBRA. Despite such difference, the MIs obtained by the pyrosequencing analysis for CG5–CG7 and CG9 and by the COBRA for CG5 and CG16 were invariably below the normal range in the same 43 patients (cases 1–43) (group 1). By contrast, the MIs were almost invariably within the normal range in the remaining 95 patients, while the MIs obtained by the pyrosequencing analysis slightly (1–2%) exceeded the normal range in the same three patients (cases 136–138).

In the 43 cases of group 1, microsatellite analysis for four loci at the telomeric 11p region excluded maternal upd in 14 cases in whom parental DNA samples were available; in the remaining 29 cases, microsatellite analysis identified two alleles for at least one locus, excluding maternal uniparental isodisomy for this region. Furthermore, oligoarray CGH for the chromosome 11p15.5 region showed no copy number alteration such as duplication of maternally derived *H19*-DMR and deletion of paternally derived

Table 1. The methylation indices (%) for the *H19*-DMR.

	Cases 1–43	Cases 44–138	Control subjects
Pyrosequencing analysis			
CG5	4–24	35–50	33–48
CG6	5–26	36–53	34–51
CG7	4–24	35–49	30–47
CG9	5–23	34–48	30–46
COBRA			
CG5 (*Hpy*188I)	3.3–35.1	37.8–60.8	36.2–58.5
CG16 (*Afl*III)	4.1–35.0	43.0–59.4	38.7–60.0

The position of examined CpG dinucleotides (CG5–7, CG9, and CG16) is shown in Figure 1A.
COBRA: combined bisulfite restriction analysis.
doi:10.1371/journal.pone.0060105.t001

H19-DMR. For the KvDMR1, the MIs of the 138 patients remained within the reference range (Fig. S1B and C).

Identification of upd(7)mat

Methylation analysis for the *MEST*-DMR revealed that unmethylated bands were absent from eight patients and remained faint in a single patient (cases 44–52) (group 2) (Figure 2B). Subsequent microsatellite analysis confirmed upd(7)mat in the eight patients and mosaic upd(7)mat in the remaining one patient, and indicated trisomy rescue or gamete complementation type upd(7)mat in cases 44–48, monosomy rescue or post-fertilization mitotic error type upd(7)mat in cases 49–51, and post-fertilization mitotic error type mosaic upd(7)mat in case 52 (Table S2).

Multiple DMR analysis

We examined 17 autosomal DMRs other than the *H19*-DMR in 14 patients in group 1, four patients in group 2, and 20 patients in group 3, and the *XIST*-DMR in eight female patients in group 1, one female patient in group 2, and five female patients in group 3 (Table S3). The MIs outside the reference ranges were identified in five of 14 examined cases (35.7%) and six of a total of 246 examined DMRs (2.4%) in group 1. In particular, a single case with the mean MI value of 23 obtained by the pyrosequencing analysis for CG5–CG7 and CG9 had an extremely low MI for the *ARHI*-DMR (case 13 of group 1). This extreme hypomethylation was confirmed by bisulfite sequencing, and direct sequencing showed normal sequences of the primer-binding sites, thereby excluding the possibility that such an extremely low MI could be due to insufficient primer hybridization because of the presence of a nucleotide variation within the primer-binding sites (Figure 3). Furthermore, no copy number variation involving the *ARHI*-DMR was identified by CGH analysis using a genomewide catalog array. Consistent with upd(7)mat, three DMRs on chromosome 7 were extremely hypermethylated in four examined cases of group 2. Only a single DMR was mildly hypermethylated in a total of 345 examined DMRs in group 3. The abnormal MIs, except for those for the *H19*-DMR in group 1 and for the three DMRs on chromosome 7 in group 2, were confirmed by three times experiments.

Oligonucleotide array CGH

A ~3.86 Mb deletion at chromosome 17q24 was identified in a single patient (case 73 of group 3) (Figure 4).

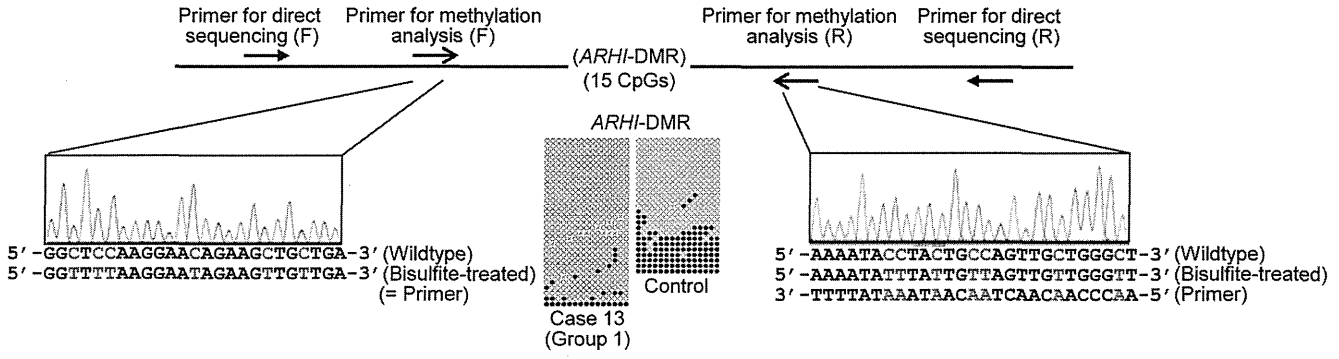

Figure 3. Analysis of the *ARHI*-DMR in case 13. For bisulfite sequencing, each line indicates a single clone, and each circle denotes a CpG dinucleotide; the cytosine residues at the CpG dinucleotides are usually unmethylated after paternal transmission (open circles) and methylated after maternal transmission (filled circles). Electrochromatograms delineate the sequences of the primer binding sites utilized for the methylation analysis.
doi:10.1371/journal.pone.0060105.g003

Epigenotype-phenotype analysis

Clinical findings of SRS patients in groups 1–3 are summarized in Table 2. All the patients met the mandatory criteria, and most patients in each group had severely reduced birth length and weight (both≤−2 SDS). For the five clinical features utilized as scoring system criteria, while 23.2% of patients in group 1 and 22.2% of patients in group 2 exhibited all the five features, there was no patient in group 3 who was positive for all the five features. By contrast, while 39.5% of patients in group 1 and 33.3% of patients in group 2 manifested just three of the five features, 77.6% of patients in group 3 were positive for just three features. In particular, the frequencies of relative macrocephaly at birth and body asymmetry were low in group 3, while those of the remaining three scoring system criteria including prominent forehead during early childhood were similar among groups 1–3.

Phenotypic comparison between groups 1 and 2 revealed that birth length and weight were more reduced and birth OFC was more preserved in group 1 than in group 2, despite comparable gestational age. In the postnatal life, present height and weight became similar between the two groups, whereas present OFC became significantly smaller in group 1 than in group 2. Body asymmetry and brachydactyly were more frequent and speech delay was less frequent in group 1 than in group 2. Placental weight was similar between the two groups, and became more similar after excluding case 52 with mosaic upd(7)mat (see legends for Table 2). Parental age at childbirth was also similar between the two groups. In group 2, placental weight was grossly similar among examined cases, as was parental age at childbirth (see legends for Table 2).

Case 13 with an extremely low MI for the *ARHI*-DMR and case 73 with a cryptic deletion at chromosome 17q24 had no specific phenotype other than SRS-like phenotype (Table S4). However, of the five clinical features utilized as scoring system criteria, all the five features were exhibited by case 13 and just three features were

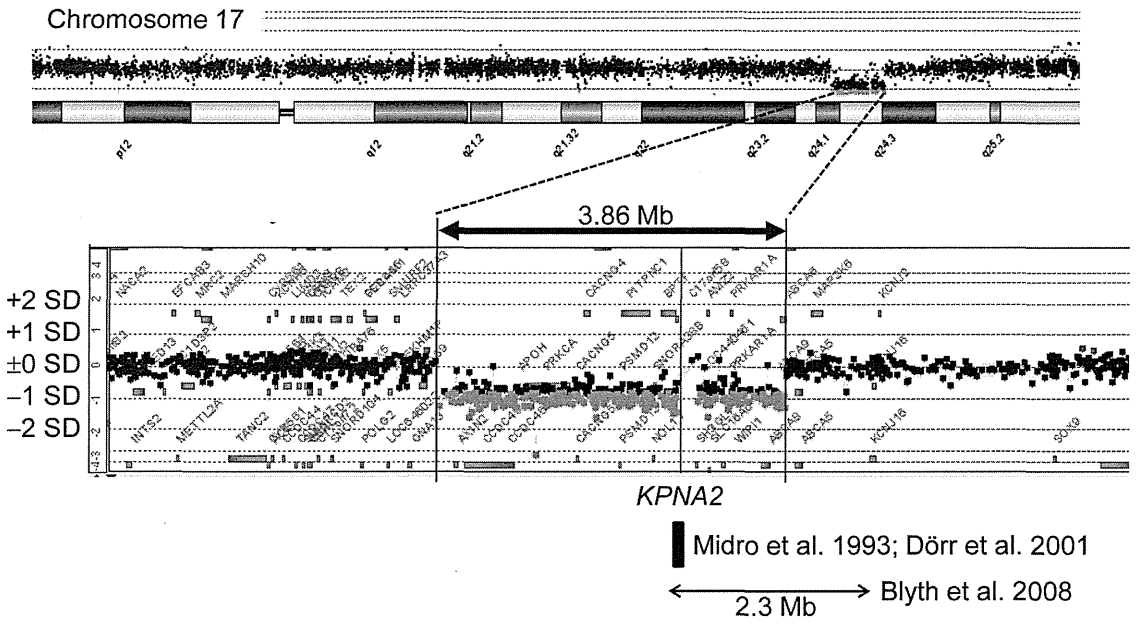

Figure 4. Oligonucleotide array CGH in case 73, showing a ~3.86 Mb deletion at chromosome 17q24. The black, the red, and the green dots denote signals indicative of the normal, the increased(>+0.5), and the decreased (< −1.0) copy numbers, respectively. The horizontal bar with arrowheads indicates a ~2.3 Mb deletion identified in a patient with Carney complex and SRS-like phenotype [44], and the black square represent a ~65 kb segment harboring the breakpoint of a *de novo* translocation 46,XY,t(1;17)(q24;q23–q24) identified in a patient with SRS phenotype [45,46].
doi:10.1371/journal.pone.0060105.g004

Table 2. Phenotypic comparison in three groups of patients with Silver-Russell syndrome.

	H19-DMR hypomethylation	Upd(7)mat	Unknown	*P*-value		
	(Group 1)	(Group 2)	(Group 3)	G1 vs. G2	G1 vs. G3	G2 vs. G3
Patient number	43 (31.2%)	9 (6.5%)	85 (62.0%)			
Mandatory criteria	43/43 (100%)	9/9 (100%)	85/85 (100%)	1.000	1.000	1.000
Scoring system criteria (5/5)	10/43 (23.2%)	2/9 (22.2%)	0/85 (0.00%)	0.965	**1.52×10^{-4}**	**2.58×10^{-2}**
Scoring system criteria (4/5)	16/43 (37.2%)	4/9 (44.4%)	19/85 (22.4%)	0.792	**1.45×10^{-2}**	0.145
Scoring system criteria (3/5)	17/43 (39.5%)	3/9 (33.3%)	66/85 (77.6%)	0.821	**7.17×10^{-4}**	0.161
Gestational age (weeks:days)	38:0 (34:3~40:0) (n = 36)	38:0 (34:4~40:0) (n = 9)	37:6 (27:1~41:4) (n = 65)	0.877	0.120	0.450
BL (SDS)	−4.13±2.01 (n = 31)	−3.18±1.16 (n = 9)	−2.93±1.43 (n = 60)	**2.67×10^{-2}**	**6.69×10^{-5}**	0.619
BW (SDS)	−3.50±0.85 (n = 42)	−2.90±0.64 (n = 9)	−2.71±1.14 (n = 64)	**3.28×10^{-2}**	**5.87×10^{-4}**	0.640
BL≤−2 SDS and/or BW≤−2 SDS*	43/43 (100%)	9/9 (100%)	85/85 (100%)	1.000	1.000	1.000
BL≤−2 SDS and BW≤−2 SDS	39/43 (90.7%)	7/9 (77.8%)	76/85 (89.4%)	0.474	0.821	0.304
BOFC (SDS)	−0.54±1.22 (n = 29)	−1.44±0.47 (n = 9)	−1.92±1.09 (n = 48)	**3.74×10^{-2}**	**1.52×10^{-6}**	0.202
BL (SDS) − BOFC (SDS)	−3.70±2.02 (n = 27)	−1.73±1.20 (n = 9)	−0.943±1.48 (n = 43)	**1.02×10^{-2}**	**3.40×10^{-9}**	0.111
BW (SDS) − BOFC (SDS)	−3.21±1.20 (n = 27)	−1.53±0.57 (n = 9)	−1.04±1.55 (n = 48)	0.326	**7.38×10^{-9}**	0.331
Relative macrocephaly at birth† BL or BW (SDS) − BOFC (SDS)≤−1.5	29/29 (100%)	7/9 (77.8%)	16/45 (35.6%)	0.341	**3.67×10^{-8}**	**2.05×10^{-2}**
Present age (years:months)	4.1 (0:6~30:6) (n = 31)	4.8 (2:4~25:2) (n = 9)	4.3 (0:1~18:6) (n = 60)	0.437	0.813	0.335
PH (SDS)	−3.58±1.65 (n = 35)	−3.77±1.13 (n = 9)	−3.17±1.50 (n = 61)	0.757	0.218	0.253
PH≤−2 SDS (≥2 years)†	29/35 (82.5%)	8/9 (88.9%)	52/61 (85.2%)	0.760	0.758	0.772
PW (SDS)	−3.15±1.16 (n = 32)	−2.77±0.76 (n = 9)	−2.77±1.34 (n = 59)	0.362	0.144	0.968
POFC (SDS)	−1.16±1.18 (n = 21)	−0.01±0.91 (n = 9)	−1.81±1.57 (n = 35)	**2.01×10^{-3}**	0.107	**3.08×10^{-3}**
PH (SDS) − POFC (SDS)	−2.47±1.63 (n = 16)	−3.62±1.38 (n = 8)	−1.55±1.82 (n = 35)	0.103	**4.39×10^{-2}**	**1.64×10^{-2}**
PW (SDS) − POFC (SDS)	−2.84±1.31 (n = 21)	−2.69±1.36 (n = 9)	−1.08±1.71 (n = 35)	0.782	**2.54×10^{-2}**	**1.90×10^{-4}**
Relative macrocephaly at present PH or PW (SDS) − POFC (SDS)≤−1.5	20/21 (95.2%)	8/8 (100%)	29/43 (67.4%)	0.223	**4.77×10^{-3}**	0.156
Triangular face during early childhood	42/43 (97.7%)	8/9 (88.9%)	65/65 (100%)	0.442	0.0773	**5.98×10^{-3}**
Prominent forehead during early childhood†	31/37 (83.8%)	7/9 (100%)	41/53 (77.4%)	0.200	0.456	0.978
Ear anomalies	14/35 (40.0%)	3/9 (33.3%)	15/55 (27.3%)	0.717	0.290	0.823
Irregular teeth	12/26 (46.2%)	4/9 (44.4%)	12/45 (26.7%)	0.930	0.0968	0.291
Body asymmetry†	30/37 (81.1%)	3/9 (33.3%)	19/59 (32.2%)	**4.77×10^{-3}**	**3.51×10^{-6}**	0.947
Clinodactyly	29/37 (78.4%)	5/9 (55.6%)	50/58 (86.2%)	0.167	0.323	**2.68×10^{-2}**
Brachydactyly	30/38 (78.9%)	2/9 (22.2%)	34/56 (60.7%)	1.16×10^{-3}	0.0642	**3.24×10^{-2}**
Syndactyly	3/36 (8.3%)	0/9 (0.00%)	3/52 (5.77%)	0.375	0.641	0.464
Simian crease	4/26 (15.4%)	2/7 (28.6%)	6/49 (12.2%)	0.429	0.705	0.252
Muscular hypotonia	17/32 (53.1%)	5/9 (55.6%)	12/50 (24.0%)	0.898	**7.49×10^{-3}**	0.0564
Developmental delay	18/37 (48.6%)	6/9 (66.7%)	25/54 (46.3%)	0.337	0.826	0.262
Speech delay	8/31 (25.8%)	6/9 (66.7%)	18/43 (41.9%)	**2.55×10^{-2}**	0.156	0.179
Feeding difficulty†	16/34 (47.1%)	6/9 (66.7%)	25/51 (49.0%)	0.301	0.860	0.333
Placental weight (SDS)	−2.10±0.74 (n = 14)	−1.72 ± 0.74 (n = 6)[a]	−1.02±0.86 (n = 18)	0.312	**4.12×10^{-3}**	**8.24×10^{-3}**
Paternal age at childbirth (years:months)	32:0 (19:0~52:0) (n = 24)	35:0 (27:0~48:0) (n = 9)	32:0 (25:0~46:0) (n = 45)	0.223	1.00	0.105
Maternal age at childbirth (years:months)	32:0 (19:0~43:0) (n = 25)	33:0 (25:0~42:0) (n = 9)[b]	30:0 (22:0~43:0) (n = 46)	0.275	0.765	0.117

BL: birth length; BW: birth weight; BOFC: birth occipitofrontal circumference; PH: present height; PW: present weight; POFC: present occipitofrontal circumference, and SDS: standard deviation score.

For body features, the denominators indicate the number of patients examined for the presence or absence of each feature, and the numerators represent the number of patients assessed to be positive for that feature.

*Mandatory criteria and †five clinical features utilized as selection criteria for Silver-Russell syndrome proposed by Netchine et al. [14].

Significant *P*-values(<0.05) are boldfaced.

[a]Placental weight SDS is −1.68, −2.55, −2.24, −1.12, −2.14 and −0.60 in case 46, 47, 49, 50, 51 and 52, respectively; the placental weight SDS is −1.95±0.57 in five cases except for case 52 with mosaic upd(7)mat.

[b]Maternal childbearing age is 32, 32, 33, 42, 32, 34, 33, 25 and 36 years in case 44–52, respectively.

doi:10.1371/journal.pone.0060105.t002

manifested by case 73. In addition, cases 136–138 with slightly elevated MIs for CG5–CG7 and CG9, and cases with multilocus methylation abnormalities, had no particular phenotype other than SRS-compatible clinical features.

Correlation analysis

In group 1, the mean value of the MIs for CG5–CG7 and CG9 obtained by pyrosequencing analysis was positively correlated with the birth length and weight, the present height and weight, and the placental weight, but with neither the birth nor the present OFC (Table 3). Such correlations with the growth parameters were grossly similar but somewhat different for the MIs obtained by COBRA (Table S5). Furthermore, the placental weight was positively correlated with the birth weight and length, but not with the birth OFC. Such positive correlations were not found in groups 2 and 3.

Discussion

The present study identified hypomethylation of the *H19*-DMR and upd(7)mat in 31.2% and 6.5% of 138 Japanese SRS patients, respectively. In this regard, the normal KvDMR1 methylation patterns indicate that the aberrant methylation in 43 cases of group 1 is confined to the *H19*-DMR. Furthermore, oligoarray CGH excludes copy number variants involving the *H19*-DMR, and microsatellite analysis argues against segmental maternal isodisomy that could be produced by post-fertilization mitotic error [26]. These findings imply that the *H19*-DMR hypomethylation is due to epimutation (hypomethylation of the normally methylated *H19*-DMR of paternal origin).

The frequency of epimutations detected in this study is lower than that reported in Western European SRS patients [1,2,14], although the frequency of upd(7)mat is grossly similar between the two populations [2,11,14,27,28]. In this context, it is noteworthy that, of the five scoring system criteria, the frequencies of relative macrocephaly at birth and body asymmetry were low in group 3, while those of the remaining three scoring system criteria were similar among groups 1–3. Since relative macrocephaly and body asymmetry are characteristic of *H19*-DMR epimutation, the lack of these two features in a substantial fraction of cases in group 3 would primarily explain the low frequency of *H19*-DMR epimutations in this study. In group 3, furthermore, the low prevalence of relative macrocephaly at birth appears to be discordant with the high prevalence of prominent forehead during early childhood. Since relative macrocephaly was evaluated by an objective method (SDS for birth length or birth weight minus SDS for birth OFC≦−1.5) and prominent forehead was assessed by a subjective impression of different clinicians, it is recommended to utilize relative macrocephaly as a more important and reliable feature in the scoring system than prominent forehead. In addition, the difference in the ethnic group might also be relevant to the low frequency of *H19*-DMR epimutations in this study.

Table 3. Correlation analyses in patients with *H19*-DMR hypomethylations.

Parameter 1	Parameter 2	*r*	*P*-value
Methylation index (%)* vs.	Birth length (SDS)	0.647	**6.70×10^{-3}**
	Birth weight (SDS)	0.590	**7.80×10^{-3}**
	Birth OFC (SDS)	0.190	0.498
	Present height (SDS)	0.612	**5.33×10^{-3}**
	Present weight (SDS)	0.605	**7.81×10^{-3}**
	Present OFC (SDS)	−0.166	0.647
	Placental weight (SDS)	0.809	**8.30×10^{-3}**
Placental weight (SDS) vs.	Birth weight (SDS)	0.717	**8.64×10^{-3}**
	Birth length (SDS)	0.636	**2.63×10^{-2}**
	Birth OFC (SDS)	0.400	0.198

SDS: standard deviation score; and OFC: occipitofrontal circumference.
*The mean value of MIs for CG5, CG6, CG7, and CG9 obtained by pyrosequencing analysis.
Significant *P*-values(<0.05) are boldfaced.
doi:10.1371/journal.pone.0060105.t003

Epigenotype-phenotype correlations in this study are grossly similar to those previously reported in Western European SRS patients [1–3]. Cases 1–43 in group 1 with *H19*-DMR epimutation had more reduced birth weight and length, more preserved birth OFC and more reduced present OFC, more frequent body features, and less frequent speech delay than case 44–52 in group 2 with upd(7)mat, although the difference in the prevalence of somatic features appears to be less remarkable in this study than in the previous studies [3,4]. This provides further support for the presence of relatively characteristic clinical features in *H19*-DMR epimutation and upd(7)mat [1–3]. In this context, previous studies have indicated biallelic *IGF2* expression in the human fetal choroid plexus, cerebellum, and brain, and monoallelic *IGF2* expression in the adult brain, while the precise brain tissue(s) with such a unique expression pattern remains to be clarified [29,30,31]. This may explain why the birth OFC is well preserved and the present OFC is reduced in group 1. However, since the difference in present OFC between groups 1 and 2 is not necessarily significant in the previous studies [32], the postnatal OFC growth awaits further investigations.

Placental weight was similarly reduced in groups 1 and 2. Thus, placental weight is unlikely to represent an indicator for the discrimination between the two groups, although the present data provide further support for imprinted genes being involved in placental growth, with growth-promoting effects of *PEGs* and growth-suppressing effects of *MEGs* [5,6]. It should be pointed out, however, that the placental hypoplasia could be due to some other genetic or environmental factor(s). In particular, while placental weight was apparently similar among cases of group 2, possible confined placental mosaicism [33,34] with trisomy for chromosome 7 may have exerted some effects on placental growth in cases with trisomy rescue type upd(7)mat.

Correlation analysis would imply that the *IGF2* expression level, as reflected by the MI of the *H19*-DMR, plays a critical role in the determination of pre- and postnatal body (stature and weight) and placental growth in patients with *H19*-DMR epimutation. Since the placental weight was positively correlated with the birth length and weight, the reduced *IGF2* expression level appears to have a similar effect on the body and the placental growth. Furthermore, the lack of correlations between the MI and birth and present OFC and between placental weight and birth OFC would be compatible with the above mentioned *IGF2* expression pattern in the central nervous system [29]. Although the MI would also reflect the *H19* expression level, this would not have a major growth effect. It has been implicated that *H19* functions as a tumor suppressor [35,36].

Multilocus analysis revealed co-existing hyper- and hypomethylated DMRs predominantly in cases of group 1, with frequencies of 35.7% of examined patients and 2.4% of examined DMRs. The results are grossly consistent with the previous data indicating that co-existing abnormal methylation patterns of DMRs are almost exclusively identified in patients with *H19*-DMR epimutation with frequencies of 9.5~30.0% of analyzed patients and 1.8~5.2% of a

total of analyzed DMRs [7–9]. Notably, the co-existing methylation abnormalities were predominantly observed as mild hypermethylations of maternally methylated DMRs and were restricted to a single DMR or two DMRs in patients with multilocus abnormalities. Such findings are obviously inexplicable not only by assuming a *ZFP57* mutation that is known to cause severely abnormal methylation patterns of multiple DMRs or a *ZAC1* mutation that may affect methylation patterns of multiple DMRs [37–39], but also by assuming defective maintenance of methylation in the postzygotic period [7]. Thus, some factor(s) susceptible to the co-occurrence of hypomethylation of the *H19*-DMR and hypermethylation of other DMR(s) might be operating during a gametogenic or postzygotic period in cases with *H19*-DMR epimutation.

The patients with multilocus methylation abnormalities had no specific clinical features other than SRS-compatible phenotype. Previous studies have also indicated grossly similar SRS-like phenotype between patients with monolocus and multilocus hypomethylations [7], although patients with multilocus hypomethylation occasionally have apparently severe clinical phenotype [7]. These findings would argue for the notion that the *H19*-DMR epimutation has an (epi)dominant clinical effect. Indeed, *H19*-DMR hypomethylation has led to SRS-like phenotype in a patient with parthenogenetic chimerism/mosaicism [21], whereas *H19*-DMR hypermethylation has resulted in Beckwith-Wiedemann syndrome-like phenotype in patients with androgenetic mosaicism [40].

An extremely hypomethylated *ARHI*-DMR was found in case 13. In this regard, it is known that *ARHI* with a potentially cell growth suppressor function is normally expressed from paternally inherited chromosome with unmethylated *ARHI*-DMR [41]. Indeed, hypermethylation of the *ARHI*-DMR, which is predicted to result in reduced expression of *ARHI*, has been identified as a tumorigenic factor for several cancers with an enhanced cell growth function [42,43]. Thus, it is possible that hypomethylation of the *ARHI*-DMR has led to overexpression of *ARHI*, contributing to the development of typical SRS phenotype in the presence of a low but relatively preserved MI of the *H19*-DMR in case 13.

Oligonucleotide array CGH identified a ~3.86 Mb deletion at chromosome 17q24 in case 73 of group 3. This provides further support for the presence of rare copy number variants in several SRS patients and the relevance of non-imprinted gene(s) to the development of SRS [10]. Interestingly, the microdeletion overlap with that identified in a patient with Carney complex and SRS-like features [44], and the overlapping region encompasses a ~65 kb segment defining the breakpoint of a *de novo* reciprocal translocation involving 17q23–q24 in a patient with SRS-like phenotype (Figure 4) [45,46]. Furthermore, the translocation breakage has affected *KPNA2* involved in the nuclear transport of proteins [46–48]. Thus, *KPNA2* has been regarded as a candidate gene for SRS, although mutation analysis of *KPNA2* has failed to detect a disease-causing mutation in SRS patients [49].

Lastly, it would be worth discussing on the comparison between pyrosequencing analysis and COBRA. Since the same 43 patients were found to have low MIs by both analyses, this implies that both methods can be utilized as a diagnostic tool. While the distribution of the MIs was somewhat different between the two methods, this would primarily be due to the difference in the employed methods such as the hybridization efficiency of utilized primers. Importantly, pyrosequencing analysis was capable of studying plural CpG dinucleotides at the CTCF6 binding site, whereas COBRA examined only single CpG dinucleotides outside the CTCF6 binding site. Thus, the MIs obtained by pyrosequencing analysis would be more accurate than those obtained by COBRA in terms of *IGF2* expression levels, and this would underlie the reasonable correlations of MIs yielded by pyrosequencing analysis with body and placental growth parameters.

In summary, the present study provides useful information for the definition of molecular and clinical findings in SRS. However, several matters still remain to be elucidated, including underlying mechanisms in SRS patients with no *H19*-DMR epimutation or upd(7)mat and the DMR(s) and imprinted gene(s) responsible for the development of SRS in patients with upd(7)mat. Furthermore, while advanced maternal age at childbirth has been shown to be a predisposing factor for the development of upd(15)mat because of increased non-disjunction at meiosis 1 [50], such studies remain fragmentary for upd(7)mat, primarily because of the relative paucity of upd(7)mat. Further studies will permit a better characterization of SRS.

Supporting Information

Figure S1 Methylation analysis of the KvDMR1 using COBRA. A. Schematic representation of the KvDMR1. A 326 bp region harboring 24 CpG dinucleotides was studied. The cytosine residues at the CpG dinucleotides are usually methylated after paternal transmission (filled circles) and unmethylated after maternal transmission (open circles); after bisulfite treatment, this region is digested with *Hpy*188I when the cytosine at the 5th CpG dinucleotide (indicated with a green rectangle) is methylated and with *Eci*I when the cytosines at the 22nd CpG dinucleotide (indicated with a pink rectangle) is methylated. *KCNQ1OT1* is a paternally expressed gene, and *KCNQ1* and *CDKN1C* are maternally expressed genes. B. Representative COBRA results. U: unmethylated clone specific bands; M: methylated clone specific bands; and BWS: Beckwith-Wiedemann syndrome patient with upd(11p15)pat. C. Histograms showing the distribution of the MIs (the horizontal axis: the methylation index; and the vertical axis: the patient number).
(TIF)

Table S1 Primers utilized in the methylation analysis and microsatellite analysis.
(XLS)

Table S2 The results of microsatellite analysis.
(XLSX)

Table S3 Methylation indices for multiple differetially methylated resions (DMRs) obtained by COBRA in 38 patients with Silver-Russell syndrome.
(XLSX)

Table S4 Clinical findings in two unique patients.
(DOC)

Table S5 Correlation analyses in patients with H19-DMR hypomethylations.
(DOC)

Acknowledgments

We would like to thank the following doctors for providing us with blood samples and clinical data: Toshio Yamazaki, Yukihiro Hasegawa, Daisuke Ariyasu, Michiko Hayashidani, Hiroshi Yoshihashi, Tomoki Kosho, Rika Kosaki, Yasuhiro Naiki, Hideki Fujita, Aya Yamashita, Katsuhiro Maeyama, Sayu Omori, Takashi Koike, Makoto Ono, Sachiko Kitanaka, Jun Mori, Shinichiro Miyagawa, Masamichi Ogawa, Toshiaki Tanaka, Naomi Hizuka, Yoko Fujimoto, Zenro Kizaki, Fumio Katsushima, Takashi Iwamoto, Wakako Yamamoto, Hotaka Kamasaki, Shun Soneda, Takahiro Tajima, Yoriko Watanabe, Kanako Ishii, Noriko Kinoshita, Tohjyu Tanaka, Eriko Nishi, Tohru Yorifuji, Yoshio Makita, Yoshinobu Honda, Junko Tsubaki, Yoko Shimabukuro, Yoko Hiraki, Kazushige

Dobashi, Kazumichi Onigata, Hisaaki Kabata, Shigeki Ishii, Kimiko Taniguchi, and Masaoki Sugita. We are also grateful to Drs. Kyoko Tanabe and Kentaro Matsuoka for their technical assistance.

Author Contributions

Conceived and designed the experiments: TF KY TO. Performed the experiments: TF KN CT S. Sano K. Matsubara MK KY. Analyzed the data: TF KN KH KY. Contributed reagents/materials/analysis tools: SM TN TH RH YM K. Muroya TK CN S. Sato TO. Wrote the paper: TO.

References

1. Eggermann T (2010) Russell-Silver syndrome. Am J Med Genet C Semin Med Genet 154C: 355–364.
2. Binder G, Begemann M, Eggermann T, Kannenberg K (2011) Silver-Russell syndrome. Best Pract Res Clin Endocrinol Metab 25: 153–160.
3. Wakeling EL, Amero SA, Alders M, Bliek J, Forsythe E, et al. (2010) Epigenotype-phenotype correlations in Silver-Russell syndrome. J Med Genet 47: 760–768.
4. Yamazawa K, Kagami M, Nagai T, Kondoh T, Onigata K, et al. (2008) Molecular and clinical findings and their correlations in Silver-Russell syndrome: implications for a positive role of IGF2 in growth determination and differential imprinting regulation of the IGF2-H19 domain in bodies and placentas. J Mol Med (Berl) 86: 1171–1181.
5. Fowden AL, Sibley C, Reik W, Constancia M (2006) Imprinted genes, placental development and fetal growth. Horm Res 65 Suppl 3: 50–58.
6. Yamazawa K, Kagami M, Ogawa M, Horikawa R, Ogata T (2008) Placental hypoplasia in maternal uniparental disomy for chromosome 7. Am J Med Genet A 146A: 514–516.
7. Azzi S, Rossignol S, Steunou V, Sas T, Thibaud N, et al. (2009) Multilocus methylation analysis in a large cohort of 11p15-related foetal growth disorders (Russell Silver and Beckwith Wiedemann syndromes) reveals simultaneous loss of methylation at paternal and maternal imprinted loci. Hum Mol Genet 18: 4724–4733.
8. Turner CL, Mackay DM, Callaway JL, Docherty LE, Poole RL, et al. (2010) Methylation analysis of 79 patients with growth restriction reveals novel patterns of methylation change at imprinted loci. Eur J Hum Genet 18: 648–655.
9. Hiura H, Okae H, Miyauchi N, Sato F, Sato A, et al. (2012) Characterization of DNA methylation errors in patients with imprinting disorders conceived by assisted reproduction technologies. Hum Reprod 27: 2541–2548.
10. Abu-Amero S, Monk D, Frost J, Preece M, Stanier P, et al. (2008) The genetic aetiology of Silver-Russell syndrome. J Med Genet 45: 193–199.
11. Hitchins MP, Stanier P, Preece MA, Moore GE (2001) Silver-Russell syndrome: a dissection of the genetic aetiology and candidate chromosomal regions. J Med Genet 38: 810–819.
12. Spengler S, Schönherr N, Binder G, Wollmann HA, Fricke-Otto S, et al. (2010) Submicroscopic chromosomal imbalances in idiopathic Silver-Russell syndrome (SRS): the SRS phenotype overlaps with the 12q14 microdeletion syndrome. J Med Genet 47: 356–360.
13. Fuke-Sato T, Yamazawa K, Nakabayashi K, Matsubara K, Matsuoka K, et al. (2012) Mosaic upd(7)mat in a patient with Silver-Russell syndrome. Am J Med Genet A 158A: 465–468.
14. Netchine I, Rossignol S, Dufourg MN, Azzi S, Rousseau A, et al. (2007) 11p15 imprinting center region 1 loss of methylation is a common and specific cause of typical Russell-Silver syndrome: clinical scoring system and epigenetic-phenotypic correlations. J Clin Endocrinol Metab 92: 3148–3154.
15. Kagami M, Yamazawa K, Matsubara K, Matsuo N, Ogata T (2008) Placentomegaly in paternal uniparental disomy for human chromosome 14. Placenta 29: 760–761.
16. Bell AC, Felsenfeld G (2000) Methylation of a CTCF-dependent boundary controls imprinted expression of the Igf2 gene. Nature 405: 482–485.
17. Hark AT, Schoenherr CJ, Katz DJ, Ingram RS, Levorse JM, et al. (2000) CTCF mediates methylation-sensitive enhancer-blocking activity at the H19/Igf2 locus. Nature 405: 486–489.
18. Takai D, Gonzales FA, Tsai YC, Thayer MJ, Jones PA (2001) Large scale mapping of methylcytosines in CTCF-binding sites in the human H19 promoter and aberrant hypomethylation in human bladder cancer. Hum Mol Genet 10: 2619–2626.
19. Fisher AM, Thomas NS, Cockwell A, Stecko O, Kerr B, et al. (2002) Duplications of chromosome 11p15 of maternal origin result in a phenotype that includes growth retardation. Hum Genet 111: 290–296.
20. Brena RM, Auer H, Kornacker K, Hackanson B, Raval A, et al. (2006) Accurate quantification of DNA methylation using combined bisulfite restriction analysis coupled with the Agilent 2100 Bioanalyzer platform. Nucleic Acids Res 34: e17.
21. Yamazawa K, Nakabayashi K, Kagami M, Sato T, Saitoh S, et al. (2010) Parthenogenetic chimaerism/mosaicism with a Silver-Russell syndrome-like phenotype. J Med Genet 47: 782–785.
22. Shaffer LG, Agan N, Goldberg JD, Ledbetter DH, Longshore JW, et al. (2001) American College of Medical Genetics statement on diagnostic testing for uniparental disomy. Genet Med 3: 206–211.
23. Hannula K, Lipsanen-Nyman M, Kontiokari T, Kere J (2001) A narrow segment of maternal uniparental disomy of chromosome 7q31-qter in Silver-Russell syndrome delimits a candidate gene region. Am J Hum Genet 68: 247–253.
24. Eggermann T, Schonherr N, Jager S, Spaich C, Ranke MB, et al. (2008) Segmental maternal UPD(7q) in Silver-Russell syndrome. Clin Genet 74: 486–489.
25. Begemann M, Spengler S, Kordass U, Schroder C, Eggermann T (2012) Segmental maternal uniparental disomy 7q associated with DLK1/GTL2 (14q32) hypomethylation. Am J Med Genet A 158A: 423–428.
26. Yamazawa K, Ogata T, Ferguson-Smith AC (2010) Uniparental Disomy and Human Disease: An Overview. Am J Med Genet C 154C: 329–334.
27. Gicquel C, Rossignol S, Cabrol S, Houang M, Steunou V, et al. (2005) Epimutation of the telomeric imprinting center region on chromosome 11p15 in Silver-Russell syndrome. Nat Genet 37: 1003–1007.
28. Bliek J, Terhal P, van den Bogaard MJ, Maas S, Hamel B, et al. (2006) Hypomethylation of the H19 gene causes not only Silver-Russell syndrome (SRS) but also isolated asymmetry or an SRS-like phenotype. Am J Hum Genet 78: 604–614.
29. Ulaner GA, Yang Y, Hu JF, Li T, Vu TH, et al. (2003) CTCF binding at the insulin-like growth factor-II (IGF2)/H19 imprinting control region is insufficient to regulate IGF2/H19 expression in human tissues. Endocrinology 144: 4420–4426.
30. Pham NV, Nguyen MT, Hu JF, Vu TH, Hoffman AR (1998) Dissociation of IGF2 and H19 imprinting in human brain. Brain Res 810: 1–8.
31. Albrecht S, Waha A, Koch A, Kraus JA, Goodyer CG, et al. (1996) Variable imprinting of H19 and IGF2 in fetal cerebellum and medulloblastoma. J Neuropathol Exp Neural 55: 1270–1276.
32. Kotzot D (2008) Maternal uniparental disomy 7 and Silver-Russell syndrome - clinical update and comparison with other subgroups. Eur J Med Genet 51: 444–451.
33. Kotzot D, Balmer D, Baumer A, Chrzanowska K, Hamel BC, et al. (2000) Maternal uniparental disomy 7-review and further delineation of the phenotype. Eur J Pediatr 159: 247–256.
34. Robinson WP (2000) Mechanisms leading to uniparental disomy and their clinical consequences. Bioessays 22: 452–459.
35. Hao Y, Crenshaw T, Moulton T, Newcomb E, Tycko B (1993) Tumour-suppressor activity of H19 RNA. Nature 365: 764–767.
36. Juan V, Crain C, Wilson C (2000) Evidence for evolutionarily conserved secondary structure in the H19 tumor suppressor RNA. Nucleic Acids Res 28: 1221–1227.
37. Arima T, Kamikihara T, Hayashida T, Kato K, Inoue T, et al. (2005) ZAC, LIT1 (KCNQ1OT1) and p57KIP2 (CDKN1C) are in an imprinted gene network that may play a role in Beckwith-Wiedemann syndrome. Nucleic Acids Res 33: 2650–2660.
38. Varrault A, Gueydan C, Delalbre A, Bellmann A, Houssami S, et al. (2006) Zac1 regulates an imprinted gene network critically involved in the control of embryonic growth. Dev Cell 11: 711–722.
39. Quenneville S, Verde G, Corsinotti A, Kapopoulou A, Jakobsson J, et al. (2011) In embryonic stem cells, ZFP57/KAP1 recognize a methylated hexanucleotide to affect chromatin and DNA methylation of imprinting control regions. Mol Cell 44: 361–372.
40. Yamazawa K, Nakabayashi K, Matsuoka K, Masubara K, Hata K, et al. (2011) Androgenetic/biparental mosaicism in a girl with Beckwith-Wiedemann syndrome-like and upd(14)pat-like phenotypes. J Hum Genet 56: 91–93.
41. Huang J, Lin Y, Li L, Qing D, Teng XM, et al. (2009) ARHI, as a novel suppressor of cell growth and downregulated in human hepatocellular carcinoma, could contribute to hepatocarcinogenesis. Mol Carcinog 48: 130–140.
42. Feng W, Marquez RT, Lu Z, Liu J, Lu KH, et al. (2008) Imprinted tumor suppressor genes ARHI and PEG3 are the most frequently down-regulated in human ovarian cancers by loss of heterozygosity and promoter methylation. Cancer 112: 1489–1502.
43. Tang HL, Hu YQ, Qin XP, Jazag A, Yang H, et al. (2012) Aplasia ras homolog member I is downregulated in gastric cancer and silencing its expression promotes cell growth in vitro. J Gastroenterol Hepatol 27: 1395–1404.
44. Blyth M, Huang S, Maloney V, Crolla JA, Karen Temple I (2008) A 2.3 Mb deletion of 17q24.2-q24.3 associated with 'Carney Complex plus'. Eur J Med Genet 51: 672–678.
45. Midro AT, Debek K, Sawicka A, Marcinkiewicz D, Rogowska M (1993) Second observation of Silver-Russel syndrome in a carrier of a reciprocal translocation with one breakpoint at site 17q25. Clin Genet 44: 53–55.
46. Dörr S, Midro AT, Farber C, Giannakudis J, Hansmann I (2001) Construction of a detailed physical and transcript map of the candidate region for Russell-Silver syndrome on chromosome 17q23-q24. Genomics 71: 174–181.
47. Cuomo CA, Kirch SA, Gyuris J, Brent R, Oettinger MA (1994) Rch1, a protein that specifically interacts with the RAG-1 recombination-activating protein. Proc Natl Acad Sci U S A 91: 6156–6160.

48. Weis K, Mattaj IW, Lamond AI (1995) Identification of hSRP1 alpha as a functional receptor for nuclear localization sequences. Science 268: 1049–1053.
49. Dörr S, Schlicker M, Hansmann I (2001) Genomic structure of karyopherin alpha2 (KPNA2) within a low-copy repeat on chromosome 17q23-q24 and mutation analysis in patients with Russell-Silver syndrome. Hum Genet 109: 479–486.
50. Matsubara K, Murakami N, Nagai T, Ogata T (2011) Maternal age effect on the development of Prader-Willi syndrome resulting from upd(15)mat through meiosis 1 errors. J Hum Genet 56: 566–571.

ARTICLE

ABSTRACT

Fibrodysplasia ossificans progressiva (FOP) is a rare disease characterized by postnatal heterotopic ossification (HO). When HO affects the masticatory muscles, mouth opening becomes restricted. This paper presents the changes in facial morphology and occlusion of a patient with FOP who was followed from the age of 8 to age 21. At the initial examination, he had a severely protruded maxilla and Angle Class II Division 1 malocclusion. His mouth opening was restricted (5.0 mm). He had a large overjet and this enabled him to clean his teeth and to eat. Orthodontic correction was not planned, and his facial growth was closely followed with attention to his oral hygiene. The maxillary protrusion and a low mandibular plane angle became more prominent as the patient aged. His mandible rotated in a counterclockwise direction. His molars had delayed eruption or were impacted and seven were extracted. His mouth opening increased slightly and his oral hygiene improved to excellent.

KEY WORDS: fibrodysplasia ossificans progressiva (FOP), heterotopic ossification, facial morphology, occlusion, growth

Facial morphology and occlusion of a patient with fibrodysplasia ossificans progressiva (FOP): a case report

Takafumi Susami, DDS, PhD;[1]* Yoshiyuki Mori, DDS, PhD;[1] Kazumi Tamura;[2] Kazumi Ohkubo, DDS, PhD;[3] Kouhei Nagahama, DDS, PhD;[4] Naoko Takahashi, DDS;[4] Natsuko Uchino, DDS;[4] Kiwako Uwatoko, DDS;[4] Nobuhiko Haga, MD, PhD;[5] Tsuyoshi Takato, MD, PhD[6]

[1]Associate Professor; [2]Oral Hygienist; [3]Assistant Professor; [4]Orthodontist—Department of Oral-Maxillofacial Surgery, Dentistry and Orthodontics; [5]Professor, Department of Rehabilitation Medicine; [6]Professor, Department of Oral-Maxillofacial Surgery, Dentistry and Orthodontics—The University of Tokyo Hospital, Tokyo, Japan.
*Corresponding author e-mail: susami-ora@h.u-tokyo.ac.jp

Spec Care Dentist 32(4): 165-170, 2012

Introduction

Fibrodysplasia ossificans progressiva (FOP) is an autosomal dominant disorder characterized by postnatal heterotopic ossification (HO).[1,2] The disorder is caused by a gene mutation in the activin A receptor type I (ACVR1), which is responsible for bone morphogenetic protein (BMP) activity.[3,4] The incidence of FOP is quite rare, affecting an estimated one in 2 million people. HO is usually not apparent at birth; congenital malformation of the great toes is a sign for early diagnosis of the disorder. HO often appears within the first decade of life, after swelling with sensation of heat and pain (flare-up) of the soft tissues such as the skeletal muscles, tendons, and ligaments. When HO occurs in tissues surrounding joints, their mobility is lost.[1,2,5-7] In the maxillofacial region, the temporomandibular joint (TMJ) and masticatory muscles are common sites of involvement and this results in restricted mouth opening.[5,8-14] Surgical treatment for the restricted mouth opening in patients with FOP often results in relapse and worsening of HO and is generally not recommended.[1,15-18] HO in growing children affects facial growth and occlusion. Although there are a few reports about occlusion,[19,20] little is known about the facial morphology and occlusion of patients with FOP. In this paper, we present a longitudinal record of facial morphology and occlusion (from 8 to 21 years of age) in a patient with FOP, and discuss the dental care for children with FOP.

Case report

The patient first visited the University of Tokyo Hospital at the age of 8 years and 9 months. He had severe maxillary protrusion in the mixed dentition with a large overjet (9.5 mm) and a deep overbite (5.0 mm). The molar relationship was Angle Class II (Angle Classification Class II, Division 1). His mouth opening was severely restricted and the maximum opening was 5.0 mm (Figure 1). Evaluation of the patient's panoramic radiograph revealed the presence of all permanent teeth, widening of the right coronoid process, and elongation of the left coronoid process; mild flattening of the bilateral condylar heads was suspected

doi: 10.1111/j.1754-4505.2012.00260.x

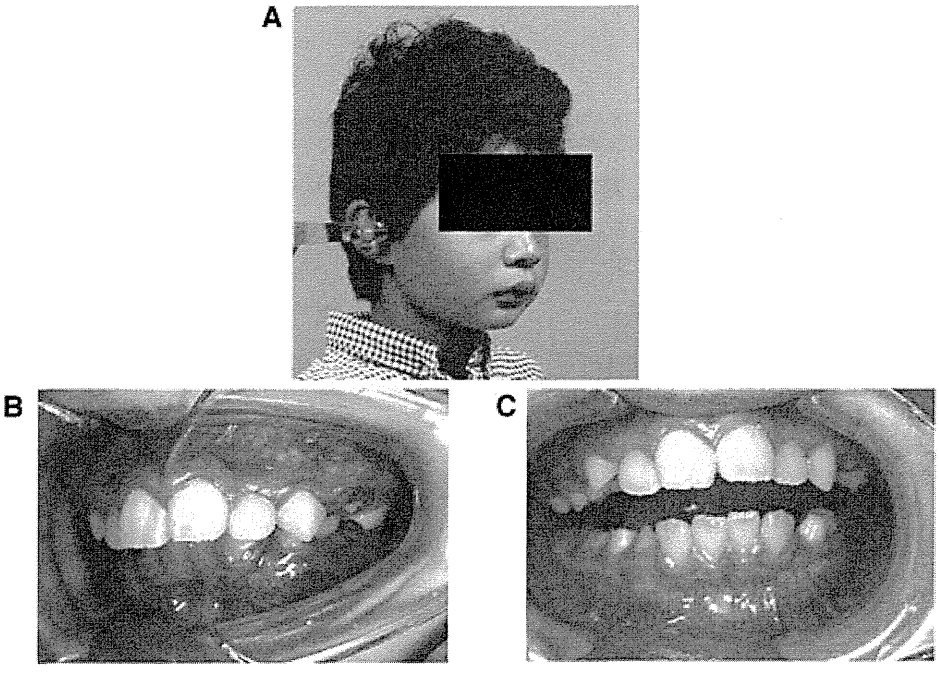

Figure 1. Facial appearance and occlusion at the initial visit (age 8 years, 9 months). (A) Face. (B) Occlusion at closed position. (C) Maximum opening. The occlusion showed severe maxillary protrusion and the amount of maximum mouth opening was 5.0 mm.

Figure 2. Panoramic radiograph at the initial visit (age 8 years, 9 months). Widening of the right coronoid process (arrow 1) and elongation of the left coronoid process (arrow 2) were seen. Mild flattening of the bilateral condylar heads was suspected (arrows 3).

(Figure 2). The lateral cephalogram showed a severe Class II facial skeleton (SNA: 85.4°, SNB: 75.6°, ANB: 9.8°) (Figure 3, Table 1). The maxilla was protruded and the mandible had normal anteroposterior development. Both maxillary and mandibular incisors were proclined and fusion of cervical vertebrae was also noted in the cephalogram. At that time, the spinal deformity in the coronal plane (scoliosis) was mild (Figure 4A).

The patient had received surgical correction of bilateral hallux valgus at the age of 1 year and was diagnosed with FOP in another hospital at 5 years of age. As the large overjet enabled his teeth to be cleaned and for him to eat, orthodontic correction was not planned and it was decided to follow his facial growth carefully and to maintain his oral hygiene at the highest level.

At 12 years of age, the patient had pain in his right hip joint, which affected

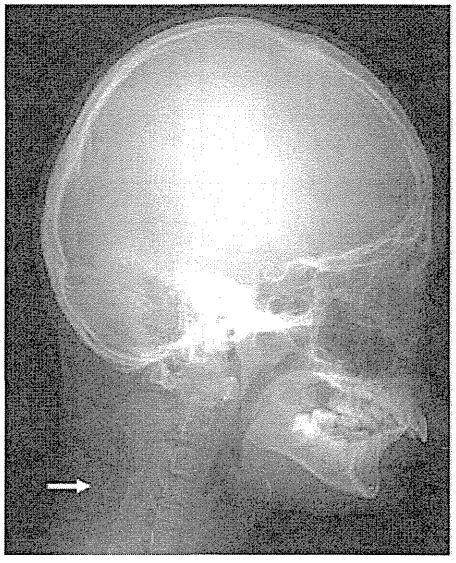

Figure 3. Lateral cephalogram at the initial visit (age 8 years, 9 months). The patient had severe Angle Class II facial skeleton. Fusion of cervical vertebrae was seen (arrow).

his movement. From 13 years of age, HO in the ligaments surrounding the vertebral column progressed, and scoliosis and tilting of the head became more prominent (Figures 4B and 5). At 16 years of age, the last cephalogram was made; as it was impossible thereafter because of his vertebral deformation. The superimposition of cephalogram tracings at ages 8 and 16 showed greater forward growth of both the maxilla and mandible relative to the anterior cranial base. The mandible showed counterclockwise rotation and both maxillary and mandibular incisors were proclined further (Figure 6, Table 1). The computed tomography (CT) made at 16 years of age clearly depicted deformation of bilateral condylar heads, widening of the right coronoid process, and elongation of the left coronoid process. HO was found at the anterior edge of the right coronoid process, but it was not fused with the upper bones of the skull (Figure 7). These findings suggested that the restricted mouth opening was caused by the mechanical interference between the coronoid processes and upper bones, and not because there was a bony fusion. Between 16 and 17 years of age, the patient experienced acute

Table 1. Cephalogram measurements.

Parameters	Age		Japanese adult male norm:
	8 years, 10 months	16 years, 4 months	Mean (SD)
SNA	85.4[a]	93.5[c]	81.8 (3.1)
SNB	75.6	81.4	78.6 (3.1)
ANB	9.8[b]	12.1[c]	3.3 (2.7)
MP-FH	19.6[a]	11.8[b]	26.3 (6.3)
U1-FH	117.9[a]	126.4[c]	108.9 (5.6)
L1-MP	123.3[c]	129.5[c]	94.7 (7.2)

MP-FH: Mandibular plane–Frankfurt plane Angle; U1-FH: Upper incisor–Frankfurt plane Aznglе; L1-MP: Lower incisor-Frankfurt plane Angle; SD: Standard deviation.
Deviation from the mean value [a]between 1 and 2 SD, [b]between 2 and 3 SD, [c]more than 3 SD.
Japanese norm is from Izuka and Ishikawa[25]

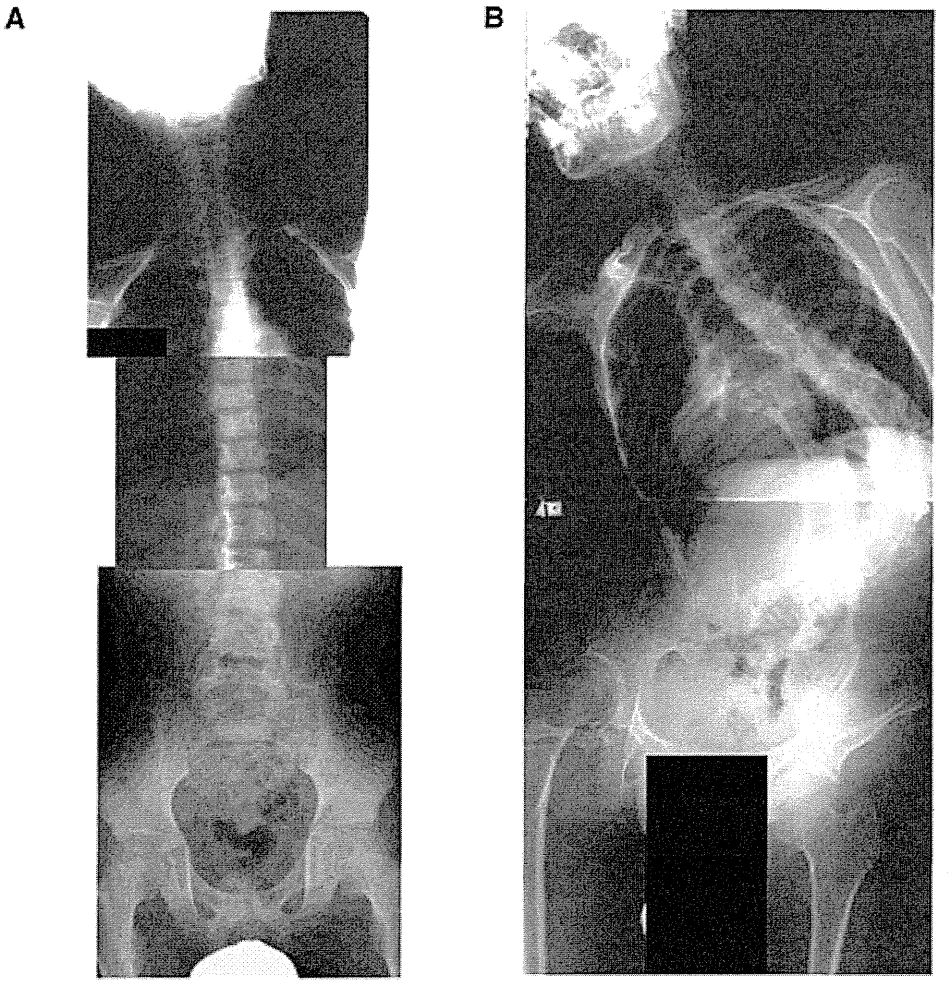

Figure 4. Integrated radiographic films of the vertebral column. (A) At the initial visit (age 8 years, 9 months). (B) At 18 years and 3 months of age, lateral curvature of the vertebral column had become severe.

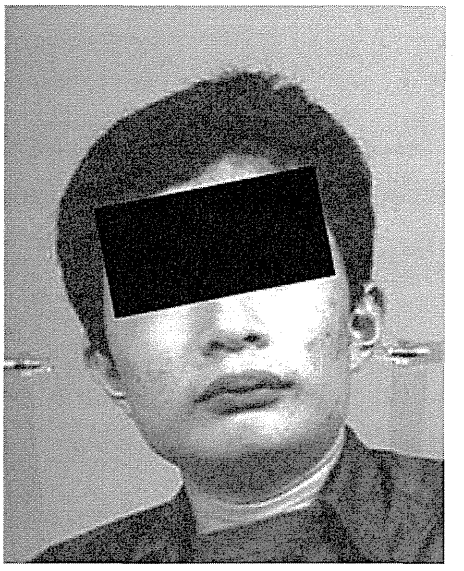

Figure 5. Facial appearance at age 15 years and 4 months. Tilting of the head had become prominent and standardization using ear rods was impossible.

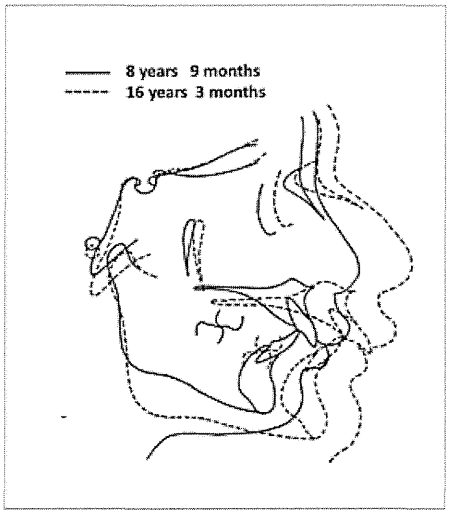

Figure 6. Superimposition of lateral cephalograms. Large forward growths of both maxilla and mandible were found. The mandible showed counterclockwise rotation and both maxillary and mandibular incisors were proclined further.

submandibular swelling (flare-up) twice and antibiotics and a bisphosphonate were administered. He also experienced swelling in the right elbow and forearm during that period.

At 19 years of age, the maxillary protrusion had increased. The overjet and overbite had increased to 12.0 and

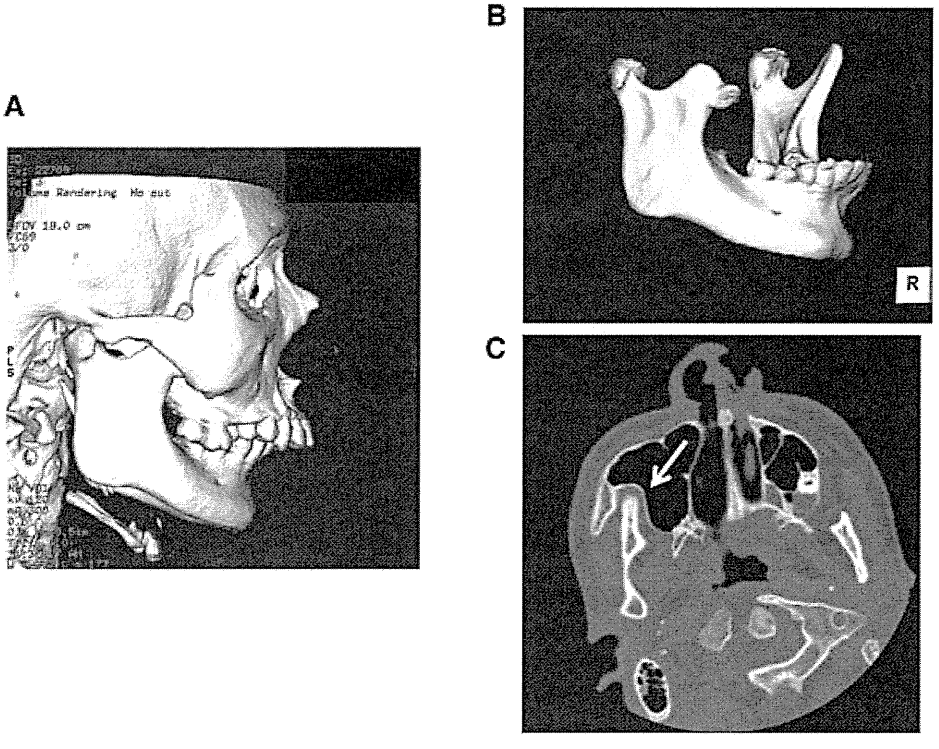

Figure 7. CT made at age 16 years and 3 months. (A) 3-D lateral facial view. (B) Extracted mandible. (C) 2-D view showing HO at the front edge of the right coronoid process. Deformation of bilateral condylar heads, widening of the right coronoid process, and elongation of left coronoid process were observed. HO was found at the anterior edge of the right coronoid process, but it was not fused with upper bones.

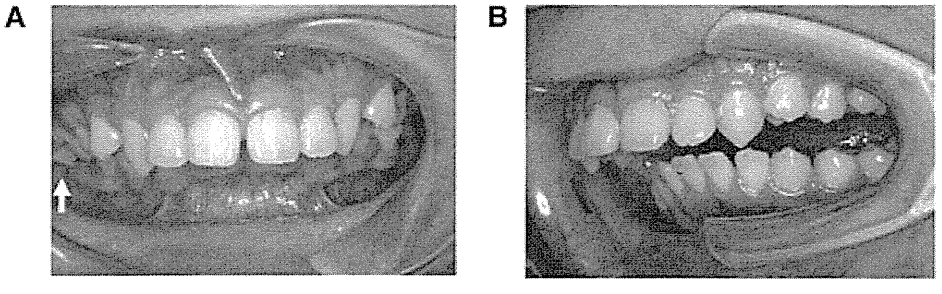

Figure 8. Occlusion at age 19 years and 4 months. (A) In occlusion. Upper right second molar had erupted buccally, showing a scissor bite (arrow). (B) Maximum opening. The maxillary protrusion deteriorated but the amount of mouth opening had slightly improved (6.0 mm).

6.0 mm, respectively. The premolars had erupted normally, but molars had delayed eruption or impaction (Figures 8 and 9). However, the amount of maximum opening slightly improved (6.0 mm). To prevent acute inflammation and subsequent swelling (flare-up) caused by dental caries or periodontal disease, seven molars were extracted under local or general anesthesia. The details of the surgical extraction of the six molars under general anesthesia have been reported previously.[21] The last examination of the patient for this report was at 21 years of age. Bone healing was good at the extraction sites and there was no further deterioration of HO in the facial region. His oral hygiene was excellent and we continue to provide periodic care.

Discussion

Signs or symptoms of FOP are usually not apparent at birth except for the congenital malformation of the great toes; HO often appears within the first decade of life after flare-ups in the soft tissues.[1,2,5,6] When joints are affected by HO, they lose their mobility, and when the vertebral column is affected, it often results in lateral curvature of the column.[1,2,7,12] TMJ and masticatory muscles are also commonly affected, resulting in restricted mouth opening.[5,8-14] The involvement of these tissues occurs relatively late in comparison with other joints, but restricted mouth opening occurs in about half of patients by the age of 20.[7] HO in oral regions appears after trauma or infection, but inadequate dental treatment and acute exacerbation of caries or periodontal disease have also been reported as causative factors.[10,14]

In growing children, HO seems to affect facial growth and occlusion. According to Nussbaum *et al.*,[19] there was a high incidence of mandibular hypoplasia and large overjet in patients with FOP. Renton *et al.*[22] reported flattening of the condylar heads which was found even in patients without restricted mouth opening. However, there are no detailed reports on facial morphology and occlusion, including changes with growth.

Our patient exhibited a skeletal Class II relationship with protrusion of the maxillary alveolar process. The mandible showed normal anteroposterior growth as measured by SNB angle at the age of 8 and 16 years. Flattening of condylar heads was suspected at the first examination and it was clearly seen later in the evaluation of the CT of the head and neck. The restricted mouth opening (5.0 mm) was already recorded at the initial visit. The patient's mother recalled that he had difficulty opening his mouth beginning in infancy. The widening of the right condylar process found at the initial examination was considered to be the cause of the restricted mouth opening. Evaluation of the CT scans made later revealed HO at the front edge of the coronoid process, though the coronoid process was not fused with upper facial

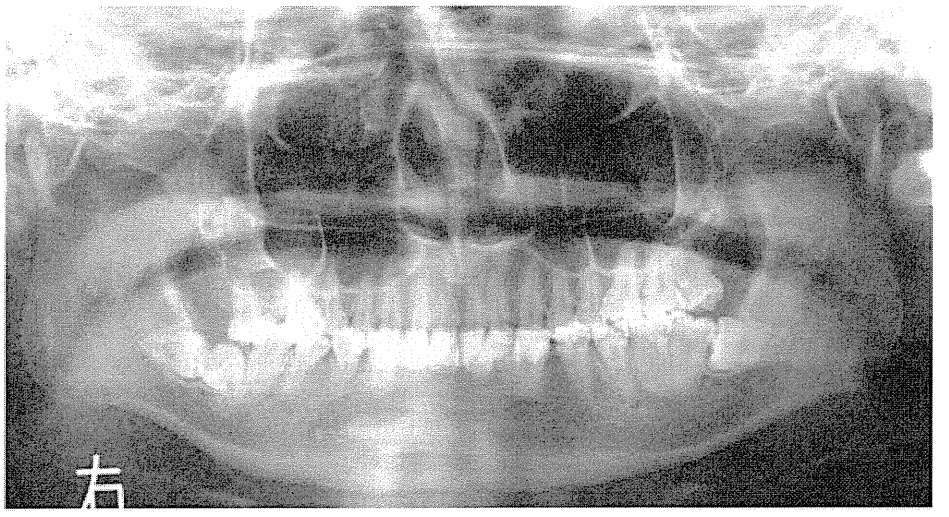

Figure 9. Panoramic radiograph at age 19 years and 5 months. Molars showed abnormal eruption or impaction. Seven molars were later extracted under local or general anesthesia.

bones (Figure 7). This suggested that the restriction was not caused by bone fusion but by mechanical interference of bones on mouth opening as pointed out by Connor and Evans[8] and Nunnelly and Yussen.[9]

Our patient had severe maxillary protrusion with Angle Class II Division 1 occlusion. As Nussbaum *et al.*[19] reported in some of their patients with FOP, this malocclusion seemed to be helpful for cleaning the oral cavity and for eating, as mouth opening was restricted in these patients. If our patient had a normal overjet, the mouth opening would have been smaller. The proclination of maxillary incisors might be caused by forces exerted during masticatory movement.

During follow-up of our patient, the mouth opening did not decrease but rather increased slightly (6.0 mm). Analysis of the cephalogram found that both the maxilla and mandible had greater forward growth than did the anterior cranial base. The ANB angle changed from 9.8° to 12.1° and the overjet changed from 9.5 to 12.0 mm. The forward inclination of both maxillary and mandibular incisors was also increased (Figure 6, Table 1). These changes indicate a probable influence on upper incisor inclination from his hyperactive lower lip as it tried to make an anterior seal during swallowing, and was also influenced by the movement of the tongue on the lower incisors as it thrusts forward to achieve an anterior seal during swallowing. Although the premolars had erupted without problem, the molars were delayed or impacted. This seemed to be due to the lack of eruption space in the posterior region of the mandibular arch. As these molars are more susceptible to dental caries and periodontal disease, seven molars were extracted under local or general anesthesia.[21] After extraction, oral hygiene maintenance became easier than before. At present, a slender toothbrush and an interdental brush are being used for oral cleaning and the patient's oral hygiene is excellent.

The guidelines for dental management of patients with FOP, such as the treatment of caries, tooth extraction, orthodontic treatment, and oral hygiene maintenance, have been proposed by several authors.[19,23] Restricted mouth opening is the main problem, but surgical release of HO has been reported to cause flare-ups and aggravate the HO further.[15] Since it is difficult to carry out dental treatment on these patients, good oral hygiene must be maintained to prevent dental caries and periodontal disease.[19,23,24] Patients should be aware of the problems with oral care methods before the onset of HO and should receive preventive or early interceptive dental treatment. However, even normal opening of the mouth during dental treatment might be traumatic for patients with FOP, and dentists caring for these patients must be aware of this problem.

Maxillary protrusion seems to be common in patients with FOP and orthodontic treatment would be safe.[10] However, the space for cleaning the mouth and eating needs be taken into consideration. If the child shows severe crowding of anterior teeth, orthodontic treatment will be helpful for maintenance of oral hygiene. However, an orthodontic appliance increases the risk of dental caries and gingivitis. Problems with posterior teeth may occur with facial growth similar to our patient, so early and regular dental examination by dentists knowledgeable about FOP is recommended. If abnormal eruption of posterior teeth is found, extraction of the teeth should be considered to prevent dental caries or periodontal disease and to avoid flare-ups and HO.

Conclusion

The patient in this case report had a severely restricted mouth opening caused by HO. He had a Class II facial skeleton and Angle Class II Division 1 occlusion. His maxilla protruded severely but his mandible showed normal anteroposterior development. He also had an abnormally low mandibular plane angle. Orthodontic treatment was not considered because the large overjet enabled him to clean his mouth and to eat. Facial growth was closely monitored over time. As the patient grew, the maxillary protrusion became more prominent and the mandible rotated counterclockwise between the ages of 8 and 16 years. However, the restricted mouth opening did not worsen. The patient's molars had delayed eruption or were impacted, and were extracted under local and general anesthesia. The patient's oral hygiene is currently excellent.

In children with FOP, involvement of the TMJ occurs rather late in comparison with other joints. If FOP is diagnosed at an early age, efforts should be made to

prevent the onset of HO. Oral hygiene maintenance and early preventive or interceptive dental treatment are necessary before the onset of HO. Orthodontic treatment to correct crowding might be helpful for oral hygiene maintenance, but the space for food intake should be taken into consideration if there is restricted mouth opening.

References

1. Kaplan FS, Le Merrer M, Glaser DL, *et al.* Fibrodysplasia ossificans progressiva. *Best Pract Res Clin Rheumatol* 2008;22:191-205.
2. Shore EM, Kaplan FS. Insights from a rare genetic disorder of extra-skeletal bone formation, fibrodysplasia ossificans progressiva (FOP). *Bone* 2008;43:427-33.
3. Shore EM, Xu M, Feldman GJ, *et al.* A recurrent mutation in the BMP type I receptor ACVR1 causes inherited and sporadic fibrodysplasia ossificans progressiva. *Nat Genet* 2006;38:525-7.
4. Kaplan FS, Xu M, Seemann P, *et al.* Classic and atypical fibrodysplasia ossificans progressiva (FOP) phenotypes are caused by mutations in the bone morphogenetic protein (BMP) type I receptor ACVR1. *Hum Mutat* 2009;30:379-90.
5. Rocke DM, Zasloff M, Peeper J, Cohen RB, Kaplan FS. Age- and joint-specific risk of initial heterotopic ossification in patients who have fibrodysplasia ossificans progressiva. *Clin Orthop Relat Res* 1994;301:243-8.
6. Kaplan FS, Xu M, Glaser DL, *et al.* Early diagnosis of fibrodysplasia ossificans progressiva. *Pediatrics* 2008;121:e1295-300.
7. Nakashima Y, Haga N, Kitoh H, *et al.* Deformity of the great toe in fibrodysplasia ossificans progressiva. *J Orthop Sci* 2010;15:804-9.
8. Connor JM, Evans DA. Extra-articular ankylosis in fibrodysplasia ossificans progressiva. *Br J Oral Surg* 1982;20: 117-21.
9. Nunnelly JF, Yussen PS. Computed tomographic findings in patients with limited jaw movement due to myositis ossificans progressiva. *J Oral Maxillofac Surg* 1986;44:818-21.
10. Luchetti W, Cohen RB, Hahn GV, *et al.* Severe restriction in jaw movement after routine injection of local anesthetic in patients who have fibrodysplasia ossificans progressive. *Oral Surg Oral Med Oral Pathol Oral Radiol Endod* 1996;81:21-5.
11. Janoff HB, Zasloff MA, Kaplan FS. Submandibular swelling in patients with fibrodysplasia ossificans progressiva. *Otolaryngol Head Neck Surg* 1996;114: 599-604.
12. Smith R. Fibrodysplasia (myositis) ossificans progressiva. Clinical lessons from a rare disease. *Clin Orthop Relat Res* 1998;346:7-14.
13. van der Meij EH, Becking AG, van der Waal I. Fibrodysplasia ossificans progressiva. An unusual cause of restricted mandibular movement. *Oral Dis* 2006;12:204-7.
14. Sendur OF, Gurer G. Severe limitation in jaw movement in a patient with fibrodysplasia ossificans progressiva: a case report. *Oral Surg Oral Med Oral Pathol Oral Radiol Endod* 2006;102:312-7.
15. Crofford LJ, Brahim JS, Zasloff MA, Marini JC. Failure of surgery and isotretinoin to relieve jaw immobilization in fibrodysplasia ossificans progressiva: report of two cases. *J Oral Maxillofac Surg* 1990;48:204-8.
16. Herford AS, Boyne PJ. Ankylosis of the jaw in a patient with fibrodysplasia ossificans progressiva. *Oral Surg Oral Med Oral Pathol Oral Radiol Endod* 2003;96:680-4.
17. Wadenya R, Fulcher M, Grunwald T, Nussbaum B, Grunwald Z. A description of two surgical and anesthetic management techniques used for a patient with fibrodysplasia ossificans progressiva. *Spec Care Dentist* 2010;30:106-9.
18. Duan Y, Zhang H, Bu R. Intraoral approach technique for treating trismus caused by fibrodysplasia ossificans progressiva. *J Oral Maxillofac Surg* 2010;68:1408-10.
19. Nussbaum BL, Grunwald Z, Kaplan FS. Oral and dental health care and anesthesia for persons with fibrodysplasia ossificans progressiva. *Clin Rev Bone Miner Metab* 2005;3:239-42.
20. Carvalho DR, Pinnola GC, Ferreira DR, *et al.* Mandibular hypoplasia in fibrodysplasia ossificans progressiva causing obstructive sleep apnea with pulmonary hypertension. *Clin Dysmorphol* 2010;19:69-72.
21. Mori Y, Susami T, Haga N, *et al.* Extraction of 6 molars under general anesthesia in patient with fibrodysplasia ossificans progressiva. *J Oral Maxillofac Surg* 2011;69:1905-10.
22. Renton P, Parkin SF, Stamp TC. Abnormal temporomandibular joints in fibrodysplasia ossificans progressiva. *Br J Oral Surg* 1982; 20:31-8.
23. Nussbaum BL, O'Hara I, Kaplan FS. Fibrodysplasia ossificans progressiva: report of a case with guidelines for pediatric dental and anesthetic management. *ASDC J Dent Child* 1996;63:448-50.
24. Young JM, Diecidue RJ, Nussbaum BL. Oral management in a patient with fibrodysplasia ossificans progressiva. *Spec Care Dentist* 2007;27:101-4.
25. Izuka T, Ishikawa F. Normal standards for various cephalometric analyses in Japanese adults. *J Jpn Orthod Soc* 1957;16:4-12.

表2 骨系統疾患国際分類(2010)和訳(Warmanら[4]より引用、改変)

グループ / 疾患名(原文)	グループ / 疾患名(和訳)	遺伝形式	MIM番号	遺伝子座	遺伝子	タンパク	注釈
1. FGFR3 chondrodysplasia group	**1. FGFR3 軟骨異形成症グループ**						
Thanatophoric dysplasia type 1 (TD1)	タナトフォリック骨異形成症1型 (TD1)	AD	187600	4p16.3	*FGFR3*	FGFR3	以前のSan Diego型を含む
Thanatophoric dysplasia type 2 (TD2)	タナトフォリック骨異形成症2型 (TD2)	AD	187601	4p16.3	*FGFR3*	FGFR3	
Severe achondroplasia with developmental delay and acanthosis nigricans (SADDAN)	重症軟骨無形成症・発達遅滞・黒色表皮腫 (SADDAN)	AD	187600を参照	4p16.3	*FGFR3*	FGFR3	
Achondroplasia	軟骨無形成症	AD	100800	4p16.3	*FGFR3*	FGFR3	
Hypochondroplasia	軟骨低形成症	AD	146000	4p16.3	*FGFR3*	FGFR3	
Camptodactyly, tall stature and hearing loss syndrome (CATSHL)	屈指・高身長・難聴症候群 (CATSHL)	AD	187600	4p16.3	*FGFR3*	FGFR3	不活性化変異
Hypochondroplasia–like dysplasia(s)	軟骨低形成症様異形成症	AD, SP					軟骨低形成症に類似するがFGFR3と非連鎖であり, おそらく異質性. 診断基準は不確定
グループ39のFGFR3関連の表現型を示すLADD症候群同様, グループ33のFGFR3変異と関連する頭蓋骨癒合症候群も参照							
2. Type 2 collagen group and similar disorders	**2. 2型コラーゲングループおよび類似疾患**						
Achondrogenesis type 2 (ACG2; Langer-	軟骨無発生症2型 (ACG2: Langer–Saldino型)	AD	200610	12q13.1	*COL2A1*	Type 2 collagen	
Platyspondylic dysplasia, Torrance type	扁平椎異形成症, Torrance型	AD	151210	12q13.1	*COL2A1*	Type 2 collagen	重症脊椎異形成症(グループ14)も参照
Hypochondrogenesis	軟骨低発生症	AD	200610	12q13.1	*COL2A1*	Type 2 collagen	
Spondyloepiphyseal dysplasia congenita (SEDC)	先天性脊椎骨端異形成症 (SEDC)	AD	183900	12q13.1	*COL2A1*	Type 2 collagen	
Spondyloepimetaphyseal dysplasia (SEMD) Strudwick type	脊椎骨端骨幹端異形成症 (SEMD) Strudwick型	AD	184250	12q13.1	*COL2A1*	Type 2 collagen	
Kniest dysplasia	Kniest骨異形成症	AD	156550	12q13.1	*COL2A1*	Type 2 collagen	
Spondyloperipheral dysplasia	脊椎末梢異形成症	AD	271700	12q13.1	*COL2A1*	Type 2 collagen	
Mild SED with premature onset arthrosis	早発性関節症を伴う軽症脊椎骨端異形成症	AD		12q13.1	*COL2A1*	Type 2 collagen	p.R719Cとp.G474S変異にしばしば関係
SED with metatarsal shortening (formerly Czech dysplasia)	中足骨短縮を伴う脊椎骨端異形成症 (以前のCzech異形成症)	AD	609162	12q13.1	*COL2A1*	Type 2 collagen	R275C変異にしばしば関係
Stickler syndrome type 1	Stickler症候群1型	AD	108300	12q13.1	*COL2A1*	Type 2 collagen	
Stickler-like syndrome(s)	Stickler様症候群						COL2A1, COL11A1, COL11A2のいずれにも非連鎖. 劣性型はCOL9A1も参照
3. Type 11 collagen group	**3. 11型コラーゲングループ**						
Stickler syndrome type 2	Stickler症候群2型	AD	604841	1p21	*COL11A1*	Type 11 collagen alpha-1 chain	
Marshall syndrome	Marshall症候群	AD	154780	1p21	*COL11A1*	Type 11 collagen alpha-1 chain	
Fibrochondrogenesis	線維性軟骨発生症	AR	228520	1p21	*COL11A1*	Type 11 collagen alpha-1 chain	
Otospondylomegaepiphyseal dysplasia (OSMED), recessive type	耳脊椎巨大骨端異形成症 (OSMED), 劣性型	AR	215150	6p21.3	*COL11A2*	Type 11 collagen alpha-2 chain	
Otospondylomegaepiphyseal dysplasia (OSMED), dominant type (Weissenbacher-Zweymüller syndrome, Stickler syndrome type 3)	耳脊椎巨大骨端異形成症 (OSMED), 優性型 (Weissenbacher–Zweymüller症候群, Stickler症候群3型)	AD	215150	6p21.3	*COL11A2*	Type 11 collagen alpha-2 chain	
グループ2のStickler症候群1型も参照.							
4. Sulphation disorders group	**4. 硫酸化障害グループ**						
Achondrogenesis type 1B (ACG1B)	軟骨無発生症1B型 (ACG1B)	AR	600972	5q32-33	*DTDST*	SLC26A2 sulfate transporter	以前はFraccaro型軟骨無発生症として知られていた
Atelosteogenesis type 2 (AO2)	骨発生不全症2型 (AO2)	AR	256050	5q32-33	*DTDST*	SLC26A2 sulfate transporter	de la Chapelle骨異形成症, McAlister骨異形成症, "新生児骨異形成症"を含む
Diastrophic dysplasia (DTD)	捻曲性骨異形成症 (DTD)	AR	222600	5q32-33	*DTDST*	SLC26A2 sulfate transporter	
MED, autosomal recessive type (rMED; EDM4)	多発性骨端異形成症, 常染色体劣性型 (rMED; EDM4)	AR	226900	5q32-33	*DTDST*	SLC26A2 sulfate transporter	多発性骨端異形成症および偽性軟骨無形成症グループ(グループ10)も参照
SEMD, PAPSS2 type	脊椎骨端骨幹端異形成症, PAPSS2型	AR	603005	10q23-q24	*PAPSS2*	PAPS-Synthetase 2	以前の"Pakistan型". 脊椎骨端骨幹端異形成症グループ(グループ13)も参照